ABSTRACT

AVETIAN, MATTHEW ISHKHAN. Simplified MC Simulation for Coupled Neutron/Gamma Transport Through a 1-D Slab of Hydrogen-1 For Secondary Gamma Production. (Under the direction of Dr. John K. Mattingly).

Sandia National Laboratory and Oak Ridge National Laboratory have developed a training simulation environment that calculates gamma detector responses using computational photon transport. This program cannot currently calculate detector responses due to secondary photons produced by neutron capture or inelastic scatter reactions. Sandia and Oak Ridge desired a simple neutron/gamma coupled transport program that would correctly model the physics of secondary photon generation from neutron capture and inelastic scatter. This simplified program will be used in an augmented implementation of their training environment program that includes secondary photons from neutron capture and inelastic scatter. The program developed for this thesis (called SimpleMCn) uses the Monte Carlo (MC) method to simulate the history of neutron transport, secondary photon creation, and secondary photon transport. In addition to implementing unbiased (i.e. analog) transport simulations, SimpleMCn also implements neutron transport using implicit capture and forced collision biasing, and it implements a method to estimate the flux at a point (i.e., it implements a point detector tally). In order to develop the transport physics models, implement the preceding biasing options and the point detector tally, and Demonstrate these methods in a simplified program, hydrogen-1, was specifically chosen for the transport medium because it demonstrates these essential methods for secondary photon generation from neutron capture without also introducing the additional, complicated bookkeeping necessary to generate secondary photons via inelastic scatter. SimpleMCn simulates neutron transport and secondary photon production in a one dimensional slab of hydrogen-1, and the

source is modeled as a beam of mono-energetic and mono-directional neutrons, impinging on the slab. SimpleMCn, and its coupling to the counterpart photon transport code SimpleMC were verified against MCNP tallies of neutron and gamma reflection and transmission versus radial location, direction and energy. The position, direction and energy distributions of those tallies from SimpleMCn and SimpleMC matched those from MCNP for analog transport simulations, simulations involving implicit capture, forced collision biasing, and point detector tallies. Relative to analog simulations, implicit capture biasing (in an optically thick medium) increased the number of secondary photons generated by a factor of 333, and forced collision biasing (in an optically thin medium) increased the number of secondary photons generated by 1.5. These results demonstrate that SimpleMCn, coupled to SimpleMC, correctly simulates neutron transport and Secondary photon generation, and that the implicit capture and forced collision biasing methods increase the efficiency of simulation of secondary photon generation via neutron capture.

Simplified MC Simulation for Coupled Neutron/Gamma Transport Through a 1-D Slab of Hydrogen-1 For Secondary Gamma Production

by
Matthew I. Avetian

A thesis submitted to the Graduate Faculty of
North Carolina State University
in partial fulfillment of the
requirements for the degree of
Master of Science

Nuclear Engineering

Raleigh, North Carolina

2015

APPROVED BY:

_____	_____
Dr. John K. Mattingly Committee Chair	Dr. Joseph Doster

_____
Dr. Kenan Gundogdu

DEDICATION

I dedicate this work to my Mother and Family.

BIOGRAPHY

The author was born in Bryn Mawr, Pennsylvania to Suzette Avetian and is the oldest of four. The author's interest in nuclear engineering occurred in high school, watching an episode from the History Channel on Chernobyl. The fact that energy could be generated from a metal intrigued the author to the point of making this field a career. The author enrolled in Engineering Physics at the University of Arizona, where he also became one of the last nuclear reactor operators on the first commercial TRIGA reactor. The decommissioning of this noble reactor was a sad day for the author, but sometimes good things die so that something better can replace them.

After graduating from the University of Arizona, the author enrolled in graduate school at North Carolina State University. The author decided to explore the field of nuclear security which has lead to this thesis. From all this experience, the author has learned that the field of Nuclear Engineering is a complex topic embedded in both science and politics. The author is excited to see the future of both his own career path and that of the Nuclear Engineering field.

ACKNOWLEDGMENTS

I would like to thank my advisor, Dr. Mattingly, for his guidance, advice, and patience. I also wish to thank my friends and colleagues for their advice.

TABLE OF CONTENTS

LIST OF TABLES

LIST OF FIGURES

CHAPTER 1

Introduction

1.1 Motivation and Goals

Computational modeling of radiation physics is an important endeavor to many fields and applications of science and engineering. From radiation shielding to reactor design, the applications of computational radiation simulation are numerous. However, the application of computational radiation transport to radiation source location and identification for emergency response training has been limited. Sandia National Laboratory and Oak Ridge National Laboratory have developed a training simulation environment that employs computational photon transport to calculate detector responses. Currently, the program cannot calculate these responses with photons produced by neutron capture or inelastic scatter interactions. Sandia and Oak Ridge desired a simple neutron/gamma coupled transport program that will model the physics, which they could then use as a basis for the implementation in the training environment program.

It has been the goal of this thesis to develop and implement a simple Monte Carlo simulation of neutron transport with the generation of gammas from neutron capture for Sandia and Oak Ridge. The program, known as SimpleMCn, has also been benchmarked with a program known as MCNP. In addition to the simulation of neutron transport and gamma production, SimpleMCn was developed to work with another code on photon radiation simulation, SimpleMC, to determine both the neutron and photon reflection and transmission by a 1-D slab. SimpleMCn and SimpleMC, which will be referred to as SimpleMCn/g, have the purpose of generating the correct albedo and transmission results of

neutrons entering a 1-D slab of hydrogen. While other materials will be needed besides hydrogen-1 for the end application, the compilation of cross sections for other materials is primarily a book keeping endeavor. Hydrogen-1 has been specifically picked because the neutron interaction cross sections are only scatter and capture. This material choice allows the focus on proving that SimpleMCn/g is capable of correctly simulating neutrons and the secondary gammas produced from neutron capture in the slab. In addition to proving correct physical simulation, the biasing techniques of implicit capture, forced collision, and Russian roulette used in SimpleMCn will be tested as well.

1.2 Prior Work

Due to the limitations of early computers, several mathematical methods and schemes were developed in order to maximize the computational resources available. For MC radiation transport simulation, these were mainly achieved by algebraic manipulations of the original equations or using substitutions to formulate them into equations that required either fewer or less complicated calculations to obtain a result[1][2]. Such examples applicable to this work are two methods developed to sample the Klien-Nishina for Compton scatter; the Khan rejection scheme [3] and the Koblinger direct sampling method [4]. Others include the general rejection method developed by Khan [5] to sample arbitrary probability distribution functions (PDF).

Authors Park and Miller developed a random number generator in reference [6] that is considered by Press et. al. to be a good minimal generator. It will pass many statistical tests, though it has the issue of not being portable to 64-bit computers. This problem was

solved by Schrage with the development of the approximate factorization of m method in reference [7]. While the generator will suffice for many basic needs, it is not considered reliable for many applications with rare events or applications with large number of calls on the random number generator as it has a low period (2.1×10^9). Press et. al. have developed a random number generator in reference [8] that uses the Bays-Durham shuffle [9] and L'Ecuyer's method of coupling two generators in reference [10], which is the random number generator used in SimpleMCn/g.

Integration of both open and closed functions has been well described by Carnahan et. al. in reference [11]. More modern versions of these methods and coded examples are provided in [8] by Press et. al. Other methods, such as the rejection scheme developed by Kahn in [5], are further mentioned in [12].

Neutron interactions will fall into one of two primary categories; either absorption or scatter. Scatters may be either elastic, where energy and momentum are conserved, or inelastic, in which energy is not conserved and the nucleus is left in an excited state. For absorption, interactions are subdivided into either capture or fission. It is important to note that SimpleMCn currently does not simulate fission interactions, so absorption reactions are only capture [13].

The neutron interactions that result in the production of gamma rays are inelastic scatter and neutron capture. For inelastic scatter, energy from the neutron is given to the nucleus, which is left in an excited state and will relax to the ground state by emitting one or more photons [14]. Neutron capture is an interaction that will frequently result in gamma

rays, however other particles are also ejectable, such as protons, deuterons, tritons, alpha particles and other light nuclei[15]. For interactions products that relax via gamma ray emission, the relaxation will occur via a cascade of energy level transitions, meaning that multiple gammas of different energies will be emitted[13].

Photon interactions fall into two primary categories of either absorption or scatter. Scatter interactions are either Compton or coherent scattering. In coherent scatter, the photon retains its original energy, thought the direction is changed. Because no energy is lost, and it is a reaction for low energy photons, it is not modeled in SimpleMC. Compton scattering changes the direction and energy of the photon in accordance with the Klien-Nishina formula. For absorption interactions, either the photon will disappear due to photoelectric absorption, or from pair production. Pair production will only occur for photons with energies that exceed twice the rest mass energy of an electron, where the photon will dissociate into an electron and a positron [16].

Authors Everett and Cashwell provide perhaps the first practical guide to neutron MC transport in reference [17]. However due to the limits of computers at the time (1959), they do not provide an accurate nor reliable method for the simulation of thermal neutrons. In the text itself the authors state "It is impractical to deal with the actual case of a distribution of neutron energies in the thermal range, ..." [17]. However, with the progress made in computers, it eventually became practical to follow thermal neutrons. Cashwell and Carter provide a new MC transport guide in reference [18], where the free gas thermal treatment of neutrons is described.

Reference [17] by Everett and Cashwell also provides a practical guide to MC transport simulation of photons. However, with the development of better sampling techniques from the Klein-Nishina provided in references [3] and [4], Cashwell and Carter provide a more modern practical guide to MC photon simulation in reference [18].

In regards to MC biasing options, the first notable appearance of the most common biasing options appears in [18] by Carter and Cashwell. Here they discuss implicit capture, Russian roulette and forced collisions. These biasing options are also explained and expanded on in the MCNP manual [19].

The coupling of neutron and gamma transport, explained by both Carter and Cashwell [18] and the MCNP manual [19], is done by following the neutron simulation until either neutron capture or inelastic scatter occur and result in a gamma ray. These interactions are the genesis of the photon history sites, which follow the MC simulation as prescribed.

1.3 Novel Elements

The demands of the thesis required a code that would calculate the albedo and transmission versus energy and direction for both neutrons and photons from a one dimensional slab and a neutron source. This required that a simplified neutron-photon coupled Monte Carlo simulation be developed. SimpleMC, a photon transport code developed by Oak Ridge, was provided. A Monte Carlo transport code for neutrons was developed, SimpleMCn, from scratch. Since there was no immediate coupling of the two programs, SimpleMC was modified slightly to accept new input data of gamma position,

direction and energy from SimpleMCn. Figures 1 and 2 below contain flow charts that demonstrate the analog steps of neutron and photon histories in SimpleMCn/g

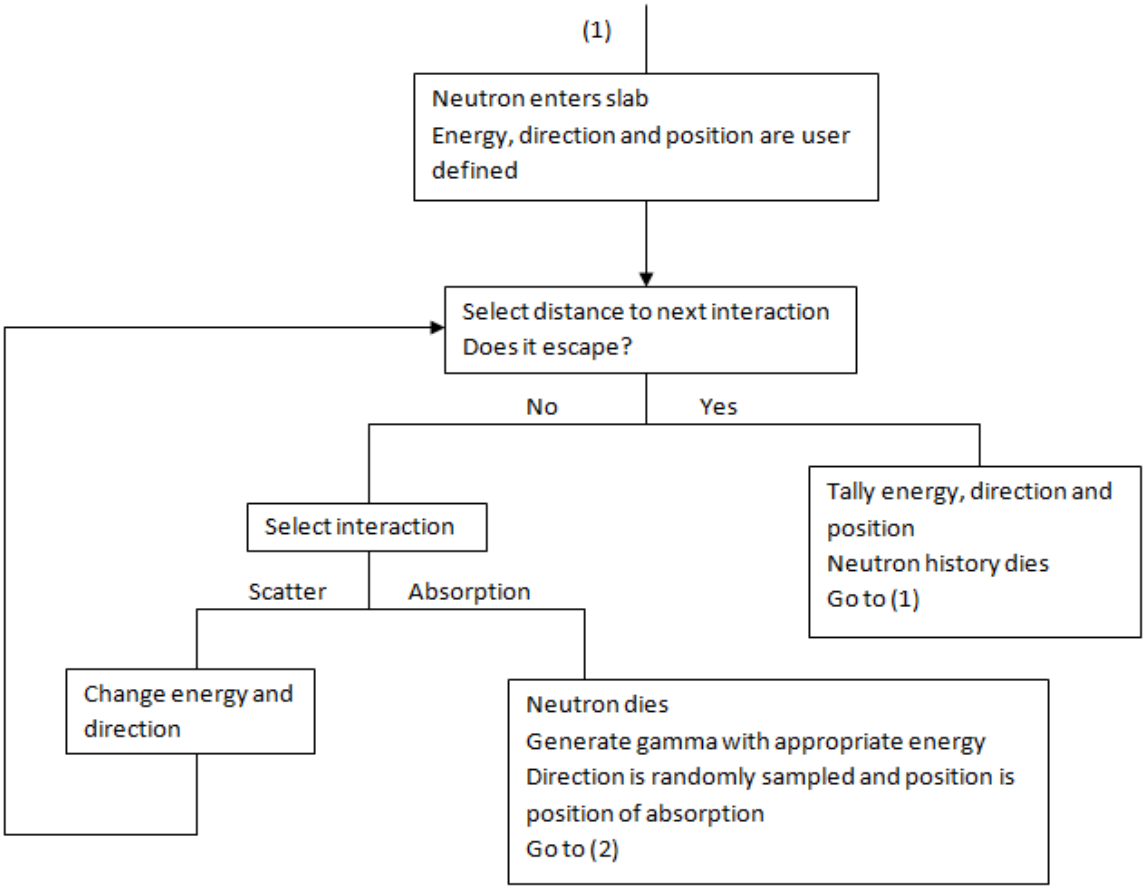

Figure 1 Flow chart showing the analog steps of neutron history in SimpleMCn.

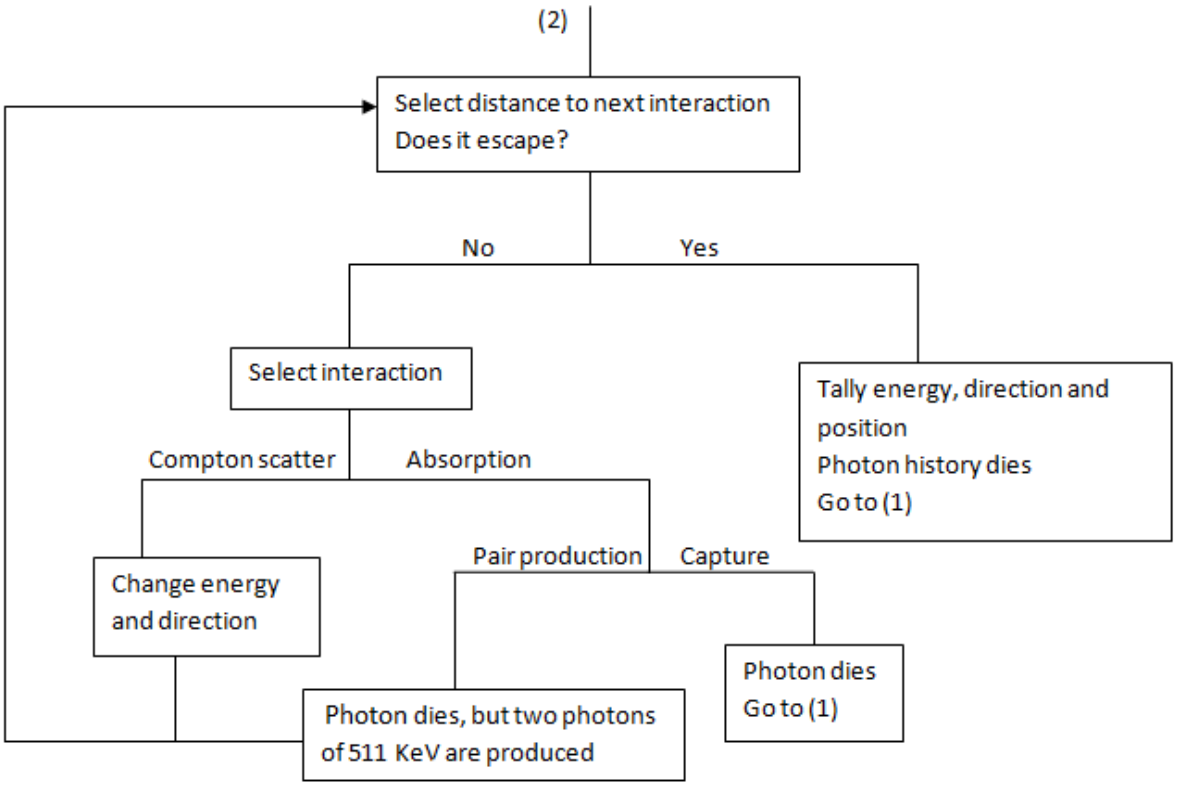

Figure 2 Flow chart illustrating the analog steps of photon history in SimpleMC.

SimpleMCn is a MC transport code designed to efficiently produce secondary gamma rays from neutron interactions in a one dimensional slab. Several basic biasing options were implemented to maximize the production of secondary gamma rays. These methods are implicit capture, where the neutron will generate a photon at each scatter, and forced collisions, where the neutrons are not allowed to escape and are required to interact inside the slab. In order to implement these biasing options without the loss of accuracy, the method of history termination known as Russian roulette was also implemented in SimpleMCn.

1.4 Organization of Thesis

This work is organized with an explanation of fundamental methods required by any Monte Carlo simulation in Chapter 2. This is followed by the physics of radiation simulation of photons and neutrons including computational recipes for the methods used in the simulation of certain properties and sampling. This chapter also covers the biasing options of implicit capture, forced collision, Russian roulette and the point detector estimator. The results of SimpleMCn/g are shown and compared to MCNP in Chapter 3 and the conclusion is provided in Chapter 4.

CHAPTER 2

Monte Carlo Simulation of Radiation Transport

Monte Carlo (MC) is a computational method in which a probabilistic model is made and a number of stochastic trials are run, from start to finish, to determine a property or solution of the model. These histories will either lead to a success or failure, which are tallied as either a 1 or 0 respectively. With a large number of histories, the mean of the successful trials will result in a statistically certain result. During a given history, properties are changed by randomly sampling from probability distribution functions (PDFs). These PDFs are usually determined by either the physics or geometry of the model. The success or failure of a history is tabulated either during the history run or at the termination, depending on the property or solution desired.

Consider finding π using the area of a unit circle inscribed in a square, the ratio of the two areas is $\pi/4$. If random points within the square were taken and all the points that were found within the circle were tallied, the ratio of accepted tallies to the total should be $\pi/4$, or about .785. If only 10 points are sampled, then 7 are expected to be accepted: $\pi/4 \approx .7$. If the number of samples is increased to 1000, then we would expect about 785 to be accepted: $\pi/4 \approx .785$. With random sampling, we are not required to get exactly the expected number of points found within the circle. It is possible to get some variation in the end result, but the more samples taken the less this variation will matter, i.e. losing or gaining a point in a sample of 10 is more catastrophic then the same loss or gain in 1000. This method of

sampling is similar to the sampling from a PDF and is an example of tallies that are taken at the end of the history.

2.1 The Random Number Generator

Random sampling is the most important process for any MC calculation, and while the sampling process may be complicated, it based on a rather simple method. A pseudo-random number from 0 to 1 is generated and then multiple mathematical manipulations are applied to select the randomly sampled result. The most important property of a random number generator is that numbers are evenly sampled between the end points of 0 and 1, which is a property to be exploited later. As one would expect, the process of picking this random number is inherently important to Monte Carlo simulations. There are multiple methods available to generate a random number and each method has different properties that make them desirable for certain applications compared to another competitive method, but ultimately the user or developer will have to decide on a generator.

While some generators are considered more robust than others [6][10][20], they all require a seed number to start the calculation. The seed number starts the random number generator calculations, and if it is the same each time, the sequence of random numbers will be entirely predictable. The most common way of selecting a random seed is to use the computer clock.

SimpleMC and SimpleMCn utilize a floating random number generator developed by Press et. al[8]. They recommend using two random number generators, both developed by L'Ecuyer[10], with a Bays-Durham shuffle [9] to develop a "perfect" generator. Both

random number generators work by taking the division and modulus of integers m and a. The equation used by both generators is known as the approximate factorization of m [7]:

$$m = aq + r \tag{2.1.1}$$

and

$$q = [m/a], r = m(\text{mod})a \tag{2.1.2}$$

where [] represents the integer part, and a and m are integers.

So that each generator is different, the a and m in one generator are not the same in the other: m_1 =2147483563, a_1 = 40014, m_2 = 2147483399, a_2 = 40692

If r<q and 0<z<m-1, where z is a given integer, then it can be shown that a(z mod q) and r[z/q] lie within 0,..,m-1, and that :

$$az \ \text{mod} \ m = \begin{cases} a(z(\text{mod})\,\text{q}) - \text{r[z/ q]} & \text{if } \geq 0 \\ a(z \ \text{mod q}) - \text{r[z/ q]} + \text{m} & \text{otherwise} \end{cases} \tag{2.1.3}$$

The shuffle's purpose is to extend the period of the random number generator. The shuffle uses an array, which is preloaded by one of the generators and both numbers from each generator are used. One is used to adjust the selected array value to get a "final" number, while the second is used to replace the array's value. This process, given in detail in Figure 1, then takes the final number and converts it into a real number between 0 and 1. The final number also seeds the next process of finding a new random number.

This three step process will evenly produce numbers from 0 to 1 without any notable dependence on the previous number. It has a large period (>$2*10^{18}$) before the number pattern is repeated. Currently, SimpleMCn/g does not use any method to adjust the initial seeding of the random number generator, which needs to be negative, so each trial will use

the same sequence of random numbers. Figure 3 provides an author generated pseudo-code of the random number generator used in SimpleMCn/g.

```
Random_number(z)                                    Z Is a negative at the start of the program
        Integers: m1=2147483563, m2=2147483399
        Integers: a1=40014, a2=40692, q1=53668, q2=52774
        Integers: r1=12211, r2=3791, ntab=32, mm1=m1-1
        Integers: ndiv=1+mm1/ntab
        Real: eps=3.0E-16, rnmx=1.0-eps, am=1.0/real(m1)
        Integers: z2=123456789, y=0
        Integer_array: v(ntab)
        Integers: j,k
        Real: temp

        Initialize
        If (z=0)
                Z
                Z2=z
                Load the shuffle table
                For(j=ntab+7, j=0, j--)          j starts at ntab+7 and is incremented down through j=0
                        K=z/q1
                        Z=a1(z-k(q1))-k(r1)
                        If( z=0)
                                Z=z+m1           Don't want it to reinitialize after this (and don't want a
                                                 negative number)
                        End if
                        If(j<ntab)               i.e. let the generator turn 7 times
                                V[j]=z
                        End if
                End for
                Y=v[0]
        End if

        Start here when not initializing
        K=z/q1
        Z=a1(z-k(q1))-k(r1)                      first generator
        If (z<0)
                Z=z+m1
        End if
        K=z2/q2
        Z2=a2(z2-k(q2))-k(r2)                    Second generator
        If (z2<0)
                Z2=z2+m2
        End if
        J=y/ndiv
        Y=v[j]-z2                                Shuffle
        V[j]=z                                   Shuffle
        If (y<1)
                Y=y+mm1
        End if
        temp=am(y)
        If (temp>rnmx)
                Return rnmx
        Else
                Return temp
        End if
End random_number
```

Figure 3 Pseudo-code for the random number generator used in SimpleMCn/g.

2.2 The Rejection Technique

Most PDFs used in MC simulation of radiation transport are not uniform over 0 to 1. One method to transform a random number into a sampled value is to use the cumulative distribution function (CDF) P(x):

$$P(x) = \int_{-\infty}^{x} p(x)dx \tag{2.2.1}$$

where p(x) represents the PDF.

An illustration of a continuous CDF, drawn from a normal distribution, is given in Figure 2, which represents the probability of finding a value of x or less.

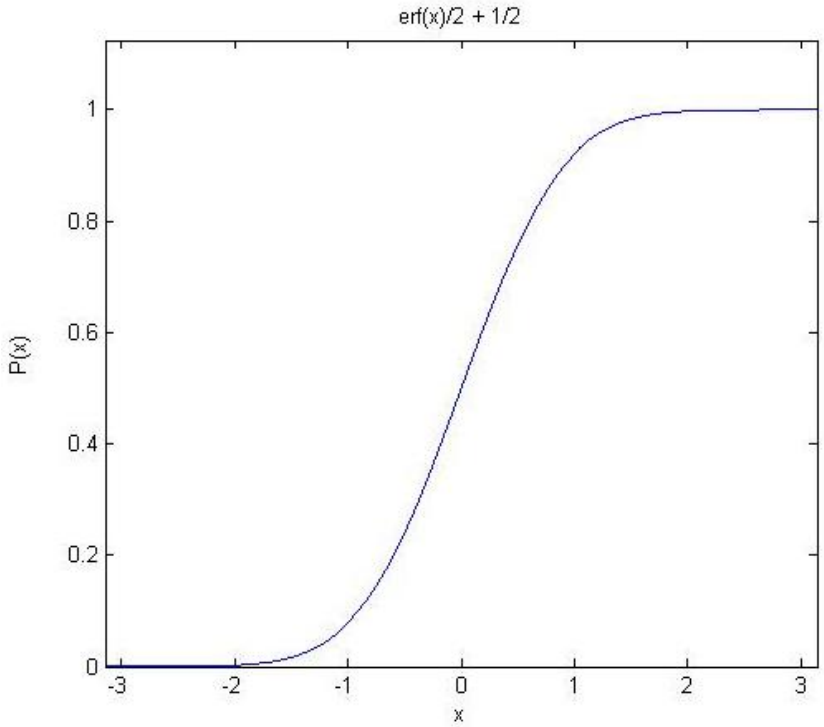

Figure 4 CDF of the normal distribution.

Since the values of P(x) are between 0 and 1, a random number ξ can be used to select an x value where equation (2.2.1) is transformed into an inverse function that yields x given ξ. Looking back at Figure 2, this would be the same as picking a spot on the y axis and then going over to the CDF and then drawing a line down to the corresponding x value.

Selecting a value using an inverse function can be computationally costly, as the math to solve an inverse function can be quite complex. An alternate method, known as the rejection technique, was developed to sample directly from the PDF. The rejection method starts with two random numbers where the first is used to find the domain position, x, of the sampling by the following equation:

$$x = a + (b - a)\xi_1 \tag{2.2.2}$$

where a is the lower bound of the domain, b is the upper bound, ξ_1 is the random number and x is the resulting randomly sampled value.

The second is used to find the range value, y:

$$y = y_{\max}\xi_2 \tag{2.2.3}$$

The resulting range value, y, must be less than the PDF's value for the sampled domain value, x, to be accepted (see Figure 5). If it is not below this value, the process is repeated, starting with two new random numbers, until there is an accepted domain value. x then becomes the sampled value for that step of the simulation. From this method, one can tabulate the frequency of sampling each possible value of the property and the resulting distribution (provided enough histories are sampled) will be the PDF. In other words, the

rejection technique will turn random numbers from a random number generator into pertinent history values.

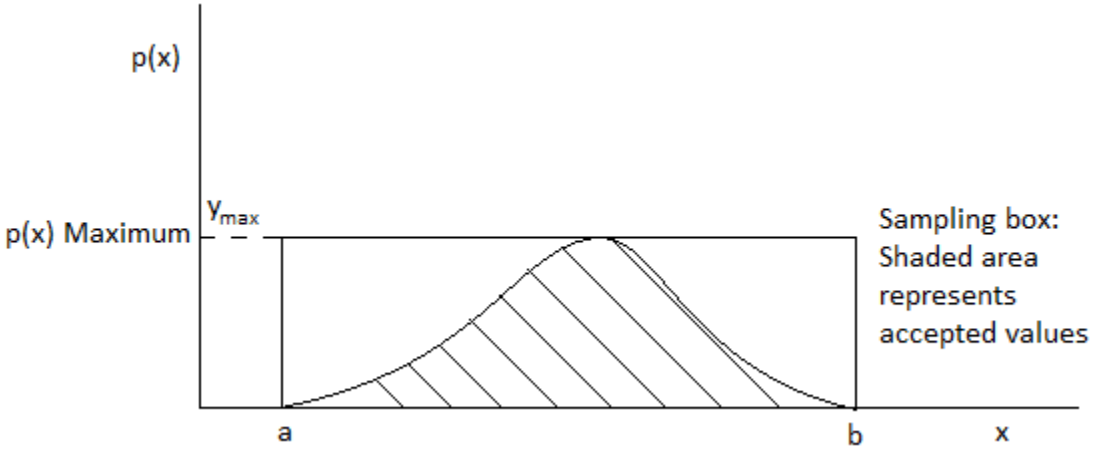

Figure 5 Illustration of the rejection technique. x is used to determine the domain value, y is used to determine the range value. If y is less than p(x) then x becomes the sampled value.

There are other techniques, such as importance functions, and dividing a single PDF into two so that efficiency of sampling an accepted value goes up. While these methods are useful in MC, they were not used in this work [12][19][21].

2.3 A General Particle History

In neutron-photon coupled MC radiation transport, there are several layers of complexity that are present due to the different physical interactions exhibited by neutrons and photons. The general steps for both sets of particles are fundamentally the same. However, physical properties like cross sections and scatter angle selection are significantly

different. In addition, when a neutron's energy drops to thermal, the energy it carries is similar in magnitude to the energy of the nuclei in the slab. This results in the possibility of an upscatter in the neutron's energy, which is an interaction that doesn't occur for photons or for neutrons at high energy. This is treated through an approximation that is exclusive to the neutron portion of the MC calculation.

Before beginning the discussion of the basic structure of MC for radiation, it would be prudent to discuss the setup of the test case for SimpleMC and SimpleMCn. A source of mono-directional mono-energetic neutrons of 1 MeV are sent into a 10 cm slab of hydrogen-1 at an angle of 90^{o} from the slab plane. For reasons that will be explained later, two cases were modeled: an "optically thick" slab (i.e. one that is many mean free paths thick), where the density is 1g/cc, and an "optically thin" slab (i.e. one that is only 1 mean free path think), where the density is 0.03g/cc. A mean free path is defined as the average distance at which the particle will interact, which is

$$\frac{1}{\Sigma}$$

where Σ is the interaction cross section.

All the above properties are user definable; the above settings were chosen for the testing of SimpleMCn/g. Please see Figure 6 for an illustration of the test case model.

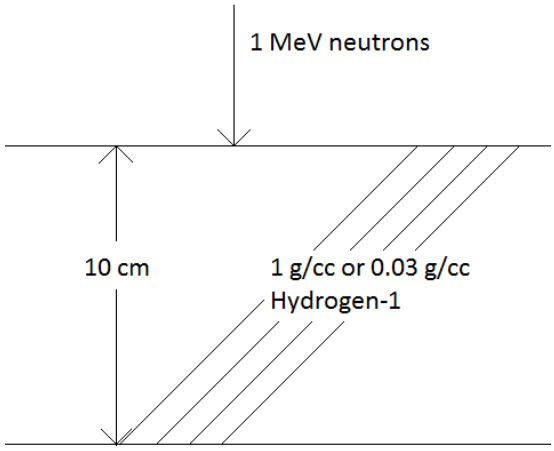

Figure 6 The test case for the coupling of SimpleMCn and SimpleMC

Interactions in the slab will result in neutrons that either emerge as reflected or transmitted, or they will be absorbed within the slab. The neutrons lost through neutron capture will generate the secondary gammas subsequently used in SimpleMC. These secondary gammas then continue through their interactions to be tallied as either a reflection or transmission (from the perspective of the neutron source).

As the particle's history is simulated, it will interact with the medium. For both SimpleMC and SimpleMCn, the position of the interaction is determined by using the total cross section of the material and a random number to determine the distance from the current position along the particle's current direction [19]. The probability of an interaction happening between L and L+dL is:

$$p(\mathrm{L})\,\mathrm{dL} = \mathrm{e}^{-\Sigma_t L}\,\Sigma_t dL \tag{2.3.1}$$

were L is the path length and Σ_t is the total cross section.

Taking the CDF, the random number is equal to:

$$\xi = \int_0^L e^{-\Sigma_t s}\Sigma_t ds = 1 - e^{-\Sigma_t L} \tag{2.3.2}$$

From this it follows that the path length is:

$$L = -\frac{log\left(1-\xi\right)}{\Sigma_t} \tag{2.3.3}$$

The interaction type is then determined by taking the ratio of the cross sections to the total cross section and placed so that they form segments of a number line from 0 to 1. A random number is generated and its position on the number line determines the interaction type. See Figure 5 for an illustration of this sampling method.

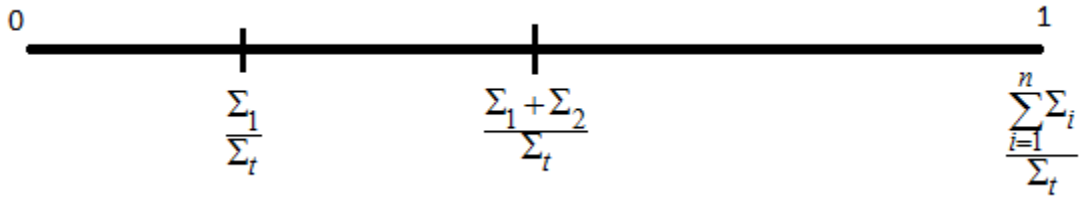

Figure 7 An example of how a cross section is selected. If the value of the random number falls between Σ_{i-1}/Σ_t and Σ_i/Σ_t then the interaction associated with Σ_i is selected.

All interactions fall into two general categories, scatter and absorption. If absorption occurs, the particle's history is terminated and the necessary properties are tabulated. In the

case of SimpleMCn/g, only histories resulting in a reflection or transmission result in tallies. After the history has been terminated and tabulated, a new particle is sampled from the start of the simulation.

If the interaction is a scatter, then the history is continued, however, the particle's energy and direction have now changed. These properties are usually interrelated, and generally the scatter angle is found first. Most commonly, the scatter angle is sampled from a PDF, and this scatter then determines the energy of the scattered particle.

One issue that is true for all scatter interactions is that the polar scatter angle is found with respect to the incident particle's direction. The polar scatter angle and the azimuthal angle are used with a rotation algorithm to find the new particle's direction. Since the azimuthal angle is independent of the polar angle, it is sampled from a uniform distribution between 0 and 2π radians:

$$\psi_s = 2\pi\xi \tag{2.3.4}$$

The rotation yields the following equations [18]:

$$\cos(\theta') = \cos(\theta_s)\cos(\theta) + \sin(\theta_s)\sin(\theta)\cos(\psi_s) \tag{2.3.5}$$

$$\psi' = \psi + \cos^{-1}\left[\frac{\cos(\theta_s) - \cos(\theta)\cos(\theta')}{\sin(\theta)\sin(\theta')}\right] \tag{2.3.6}$$

where θ' is the new polar direction, ψ' is the new azimuthal direction, θ is the original polar direction, ψ is the original azimuthal direction, θ_s is the polar scatter angle, and ψ_s is the azimuthal scatter angle given in (2.3.4).

The direction cosines are determined from:

$$u' = u\cos(\theta_s) + \frac{uw\sin(\theta_s)\cos(\psi_s) - v\sin(\theta_s)\sin(\psi_s)}{\sqrt{1-w^2}} \tag{2.3.7}$$

$$v' = v\cos(\theta_s) + \frac{vw\sin(\theta_s)\cos(\psi_s) - u\sin(\theta_s)\sin(\psi_s)}{\sqrt{1-w^2}} \tag{2.3.8}$$

$$w' = w\cos(\theta_s) - \sin(\theta_s)\cos(\psi_s)\sqrt{1-w^2} \tag{2.3.9}$$

where u, v, and w are the original x, y, and z direction cosines and u', v', and w' are the x, y, and z scatter direction cosines, respectively.

2.4 Photons

Because photons are neutral and massless particles, they are physically the simplest of the two radiation particles. Photons will primarily interact with either the atom as a whole, the nucleus, or with individual electrons, and have three interactions important to accurate simulation: photoelectric absorption, pair production, and Compton scatter. The following sections present the physical description of each process and how they are modeled in SimpleMC.

2.4.1 Photoelectric Absorption

In photoelectric absorption, the photon interacts with the atom as a whole, wherein the photon will entirely disappear. The atom releases the excess energy by ejecting an electron with the energy of the photon minus the binding energy of the electron:

$$E_{e^-} = E_\gamma - E_b \tag{2.4.1}$$

In SimpleMC this process terminates the existence of the photon, meaning that the particle's MC history ends.

The resulting vacancy in the atom maybe filled by a free electron or by a higher orbital electron where one or more characteristic X-rays may be generated. Because these X-rays are usually reabsorbed close to the generation point, through photoelectric absorption, they are not modeled in SimpleMC.

2.4.2 Pair Production

Pair production is an interaction type that occurs to photons with an energy above twice the electron rest mass, 1.022 MeV. If such a photon passes near the nucleus, it has the opportunity to dissociate into an electron and a positron. Any excess energy above 1.022 MeV will be shared between the particles and the recoil nucleus. While the electron will pass through the medium as a free electron, the positron will interact with another electron and annihilate, usually within the immediate vicinity of its birth. This then creates two photons of 0.511 MeV (rest-mass energy of an electron/positron) that, to conserve momentum, travel in opposite directions [16][22].

In SimpleMC, pair production is simplified to the termination of the incoming photon and the emergence of two annihilation photons, starting in the same position of the incident photon. This is an acceptable approximation because the positron annihilates near its generation point. To avoid tracking multiple particles, the pair production photons in SimpleMC are modeled as “one” photon, although the weight (a feature discussed later) is multiplied by 2. Since the direction selection is isotropic, with a large number of histories the average result will be the same as if both photons were tracked individually. This allows the two photons to be modeled by one particle which now has twice the importance as before.

The direction of the photon is sampled randomly and the rest of its history continues unaltered.

2.4.3 Compton Scatter

Compton scatter is the process in which a photon interacts with an electron, but unlike in photoelectric absorption, only a portion of the photon's energy is imparted into the electron. The electron is assumed to be at rest, and the photon is scattered through an angle, θ, from the original direction, see Figure 6. Since the scatter angle can vary from 0 to π radians, the energy lost from the photon can be anywhere from 0 to a significant fraction of the photon's incident energy. Naturally, the lost energy is imparted to the electron, which goes through a recoil angle determined by the conservation of momentum [16].

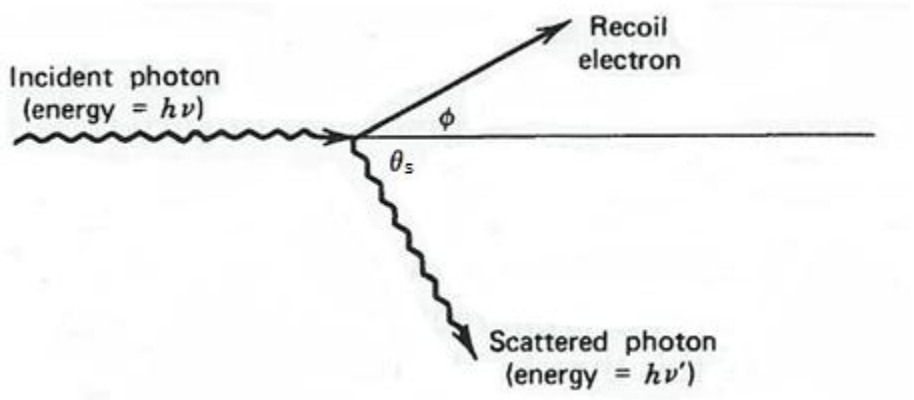

Figure 8 Illustration of a Compton scatter interaction taken from [16].

The equation for the scattered photon's energy, the Compton scatter equation, is [16]:

$$E' = \frac{E}{1+\alpha\left(1-\cos\left(\theta_s\right)\right)} \tag{2.4.2}$$

where $\alpha = \frac{E}{m_e c^2}$, θ_s is the scatter angle, E is the incident energy, E' is the emergent energy, and $m_e c^2$ is the rest mass of the electron.

The angular distribution for Compton scatter is determined by the Klein-Nishina [16] formula:

$$\frac{d\sigma_c}{d\Omega} = r_0^2\left[\frac{1}{1+\alpha\left(1-\cos\left(\theta_s\right)\right)}\right]^3\left[\frac{1+\cos\left(\theta_s\right)}{2}\right]\left[1+\frac{\alpha^2\left(1-\cos\left(\theta_s\right)\right)}{\left(1+\cos\left(\theta_s\right)^2\right)\left[1+\alpha\left(1-\cos\left(\theta_s\right)\right)\right]}\right] \tag{2.4.3}$$

where, σ_c is the Compton cross section, Ω is the solid angle, and r_0 is the classical electron radius,

$$r_0 = \frac{e^2}{4\pi\epsilon_0 m_e c^2}$$

where e is the electron charge, m_e is the electron mass, and ε_o is the permittivity of free space.

In practice, directly sampling the scatter angle from the Klein-Nishina differential cross-section is difficult, so other sampling routines are used to obtain the resulting scatter angle and energy. While there are several available methods, SimpleMC only uses two of them. For energies less than 1.4 MeV, the Kahn Rejection scheme is used. For energies that are higher than 1.4, the Koblinger direct sampling method is used.

2.4.3a Kahn Rejection Method

Kahn rejection sampling draws on the ratio, r, of the Compton wavelength after the scatter, λ', to the wavelength before, λ. To implement this, we use the Klein-Nishina as a function of the wavelength[3]:

$$\sigma_c(\lambda,\lambda') = Z\pi r_e^2\left(\frac{\lambda}{\lambda'}\right)\left[\left(\frac{\lambda}{\lambda'}\right)+\left(\frac{\lambda'}{\lambda}\right)+(\lambda'-\lambda)(\lambda'-\lambda-2)\right] \tag{2.4.4}$$

where $1 \le r \le 1+\frac{2}{\lambda}$.

This can then be recast into a PDF of the initial wavelength and the ratio, where the ratio, r, is what we wish to sample:

$$f(\lambda,r) = K[A_1 g_1(r) f_1(r) + A_2 g_2(r) f_2(r)]$$

where,

$$r = \frac{\lambda'}{\lambda}$$

$$A_1 = \frac{\lambda+2}{9\lambda+2}$$

$$A_2 = \frac{8\lambda}{9\lambda+2}$$

and,

$$g_1(r) = \frac{\lambda}{2}$$

$$g_2(r) = \frac{\lambda+2}{2r^2}$$

$$K = \frac{[3(9\lambda+2)]}{[16(\lambda+2)]}$$

Since K has no dependence on r, it may be ignored. We then note that $A_1 + A_2 = 1$, and g_1 and g_2 are PDF's with conditional probability distributions (CPD):

$$G_1(r) = \frac{\lambda}{2}(r-1)\ and\ G_2(r) = \frac{\lambda+2}{2}\left(1-\frac{1}{r}\right)$$

Condition: $0<r\leq 1$

From the sampled ratio, we can determine the scatter wavelength: $\lambda' = \lambda r$ and thus the scatter energy of the photon. We can also find the scatter angle (2.4.5) and thus the new direction with equations (2.3.7)-(2.3.9).

$$\lambda' = 1 + \lambda - \cos(\theta_s) \tag{2.4.5}$$

Faw and Shultis provided a logic diagram shown below in Figure 7. Since Faw and Shultis use a different set of variables, the flow chart in Figure 7 has been modified to remain consistent the variables used in this thesis.

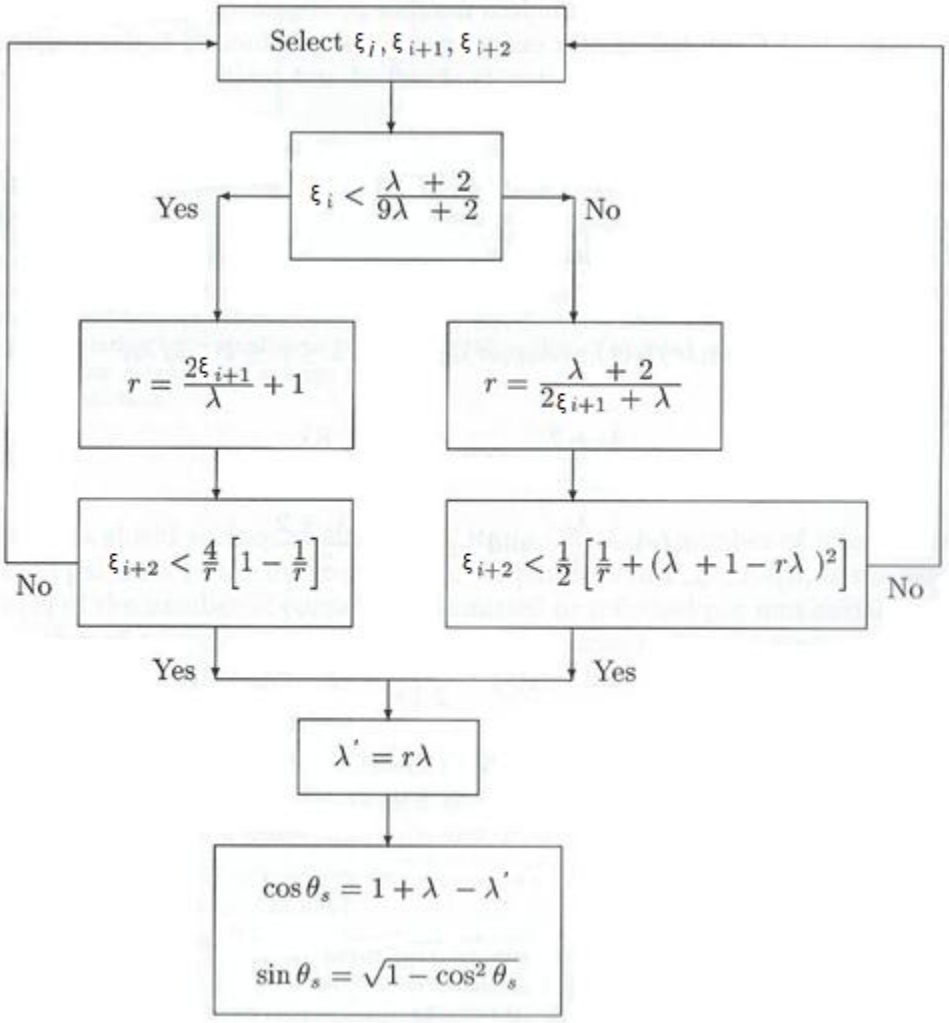

Figure 9 Kahn rejection flow chart for sampling the scatter angle of a photon from Compton scatter taken from [3].

2.4.3b Koblinger Direct Sampling Method

The Koblinger direct sampling method utilizes a theorem to efficiently find the scatter energy of the photon where other methods become inefficient or computationally costly [4]. The theorem requires a PDF with the following properties:

1) The PDF must integrate to one over all space,

$$\int_{-\infty}^{\infty} f(x)dx = 1$$

2) The PDF can be written as:

$f(x) = \sum_{i=1}^{N} \varphi_i(x)$ Where $\varphi_i(x) \geq 0, i = 1,2,3, \ldots N$

The Klein-Nishina PDF fits the requirements of this theorem when written as follows:

$$d\sigma = k(A + \frac{B}{x} + \frac{C}{x^2} + \frac{D}{x^3})$$

where $1 \leq x \leq 1 + 2\alpha$, $\alpha = \frac{E}{m_e c^2}$ and $x = \frac{\alpha}{\alpha'}$

and

$$k = \frac{\pi r_o^2}{\alpha}$$

$$A = \frac{1}{\alpha^2}$$

$$B = 1 - \frac{2(\alpha + 1)}{\alpha^2}$$

$$C = \frac{1 + 2\alpha}{\alpha^2}$$

$$D = 1$$

The condition that the PDF be greater or equal to zero puts the lower limit of 1.396 MeV on the incident photon energy. Koblinger provides greater detail of the derivation of this method, but the result is that the term for x is selected via the inequality:

$$\sum_{j=0}^{i-1} p_j(x) \leq \xi_1 \leq \sum_{j=0}^{i} p_j(x) \qquad (2.4.6)$$

where $p_i(x) = \int_1^{1+2\alpha} \varphi_i(x)dx$.

Then x is found from:

$$\frac{1}{p_i}\int_1^x \varphi_i(\psi)\,d\psi = \xi_2 \tag{2.4.7}$$

where ξ_2 is another random number independent of the random number ξ_1 in(2.4.6).

The results for each of the four terms in eq (2.4.7) are respectively,

$$x = 1 + 2\alpha\xi_2$$

$$x = \beta^{\xi_2}$$

$$x = \frac{\beta}{1 + 2\alpha\xi_2}$$

$$x = (1 - \gamma\xi_2)^{-\left(\frac{1}{2}\right)}$$

where $\beta = 1 + 2\alpha$ and $\gamma = 1 - \beta^{-2}$.

The random number ξ_2 selects how far in the integral we need to go in equation (2.4.7), where ξ_1 determines which of the terms above we use to determine x. Once the x is selected, the scatter energy is α'=α/x and the scatter angle is found by placing this in the Compton scatter equation (2.4.2) to produce:

$$\cos(\theta_s) = 1 - \frac{x - 1}{\alpha}$$

Again, the new direction cosines are found using equations (2.3.7)-(2.3.9) from earlier.

2.5 Neutrons

Similar to photons, neutrons do not possess charge. Neutrons interact directly with the nuclei of the medium. Neutron interactions with nuclei will produce one of several possible results; elastic scatter, inelastic scatter, fission, and capture. Neutron capture and inelastic scatter may generate secondary gamma rays. It is important to remember that neutron interactions that produce gamma rays are the important reactions for SimpleMCn. These gamma rays are to be used by SimpleMC and are the reason for the development of SimpleMCn. Hydrogen-1 only has two major cross sections; elastic scatter and neutron capture [23], where neutron capture will only result in the production of a secondary gamma. Hydrogen-1 was chosen for the testing of SimpleMCn because it exercises all the necessary mechanics of simulating neutron transport and secondary gamma production.

2.5.1 Neutron Capture

Neutron capture does not necessarily result in only gamma rays as secondary radiation. Neutron capture can result in the release of nucleons (e.g. (n,p) and (n,xn)) and other nuclei (e.g. deuterons, tritons, and alpha particles). However, the problem of neutron-gamma coupled transport is of particular interest for SimpleMCn/g, so this work focuses on the interactions and modeling of neutron capture that leads to secondary gamma radiation. The capture of neutrons in hydrogen-1 results in a single gamma ray of 2.223 MeV [22]. Consequently, in SimpleMCn, once a neutron is captured its history is terminated and a photon history of 2.223MeV with a randomly sampled direction is created.

2.5.2 Elastic Scatter

Although the hydrogen-1 cross-section is known exactly, there are no models that predict the scatter angle probability with respect to the incident energy [23]. For an arbitrary nucleus, experimental data tables of neutron scatter angle are provided, and the rejection technique is applied on these experimental PDFs. In hydrogen-1, neutrons with energy below 1 MeV, in the center of mass frame, have a uniform distribution for scatter cosine PDF [23]. As a result, SimpleMCn samples the scatter cosine uniformly between -1 and 1.

$$\mu = 2\xi - 1$$

After the scatter cosine is selected, the energy of the neutron is selected using the following equation:

$$E' = E\frac{(1+\alpha)+(1-\alpha)\mu}{2} \tag{2.5.1}$$

where $\alpha = \left(\frac{A-1}{A+1}\right)^2$ and A is the atomic mass of the scatter nucleus in units of neutron mass.

2.5.2a Free Gas Treatment of Thermal Neutrons

In the case of thermal neutrons, the kinetic energy of the particle is on the same order as that of the nuclei in the medium through which they interact. This occurs at around 10 kT, where k is the Boltzmann constant and T is the temperature of the medium. The consequence is that neutrons may upscatter in energy, resulting in neutrons with a longer life, more scatters, and a greater chance of escaping the medium. If this property is not accounted for, then the resulting albedo or transmission tabulations will be below the expected results. To account for this, SimpleMCn uses a method known as the free gas model for neutrons that

fall below the energy of, 9 kT, where *k* is the Boltzmann constant and T is the temperature of the slab. This method is widely used on thermal neutrons due to the fact that it can accurately produce thermal flux results without the use of look-up tables.

The free gas model works on the principle that the energy of the nuclei of the medium and the neutrons are comparable to each other so that both the neutron and the nuclei are considered energetically free, much like a gas. Due to the fact that the medium is no longer being treated as a solid, the energy-scatter selection process will change as well as the cross sections at the thermal energies. It is important to note that SimpleMCn does not currently account for neutron scatter on molecules or the crystalline structure of a material, known in MCNP as the S(α,β) method, which can occur at thermal energies as well [24]. This has not been included since it is not a reaction that would occur in a slab of hydrogen-1.

For the free gas treatment, the neutron energy and incident directions are fixed quantities entering the scatter, while the nucleus energy and the angle at which the nucleus and neutron intersect is randomly selected. The energy selection PDF for the nucleus is the Maxwell-Boltzmann distribution. Recall that the Maxwell-Boltzmann distribution does allow for particles with large, though not infinite, energy (see Figure 8), and computers have difficulty dealing with large numbers, so for practicality, the energy is limited so that the energy selection includes 99.875% of the distribution. From scattering kinematics, the new energies of both particles and scatter directions are determined [18].

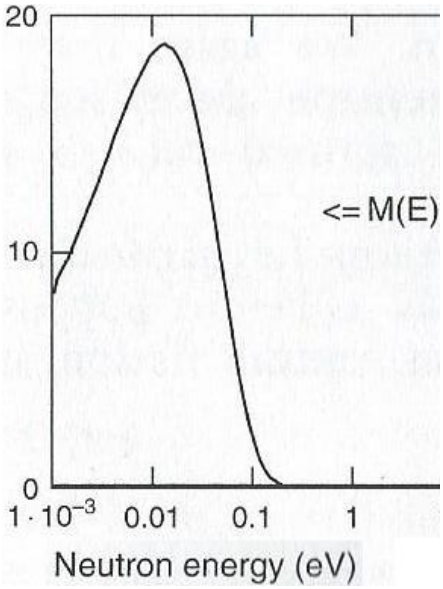

Figure 10 Illustration of the Maxwell-Boltzmann distribution of thermal neutrons taken from [13].

From the Maxwell-Boltzmann distribution,

$$M(E) = \frac{2\pi}{(\pi kT)^{3/2}} E^{1/2} e^{-(E/kT)} \tag{2.5.2}$$

we acquire the following equation for the probability of selecting the target nucleus speed, V, with a cosine of the neutron and nucleus direction vectors, μ_t :

$$p(V, \mu_t) = \frac{2}{\pi^{\frac{1}{2}}} \beta^3 V^2 e^{-\beta^2 V^2} \tag{2.5.3}$$

where $\beta = \left(\frac{A}{2kT}\right)^{\frac{1}{2}}$ and A is the mass of the target nucleus in units of the mass of a neutron.

The effective scattering cross section in the laboratory frame of reference is:

$$\sigma_s^{eff}(E) = \frac{1}{v_n} \iint \sigma_s(v_{rel}) v_{rel} p(V, \mu_t) dV d\mu_t \tag{2.5.4}$$

Where v_n is the speed of the neutron. From the cosine law, the relative velocity between the neuron and the nucleus is:

$$v_{rel} = \left[v_n^2 + V^2 - 2 v_n V \mu_t \right]^{\frac{1}{2}} \tag{2.5.5}$$

It is assumed that the scattering cross section of a nucleus is independent of the relative velocity, i.e.:

$$\sigma_s(v_{rel}) = \sigma_s^0 = constant \tag{2.5.6}$$

Going further into the calculation of the cross section, it is easier to use the dimensionless variables of

$$x = \beta V \; and \; a = \beta v_n$$

Placing (2.5.5) and (2.5.6) and the dimensionless variables into equation (2.5.4) along with several mathematical manipulations, the end result is:

$$\sigma_s^{eff}(E) = \frac{2\sigma_s^0}{3a^2\pi^{\frac{1}{2}}} \int_0^\infty \left[(a+x)^3 - |a-x|^3 \right] x e^{-a^2} dx \tag{2.5.7}$$

which, completing the integral, results in:

$$\sigma_s^{eff}(E) = \sigma_s^0 \left[\left(1 + \frac{1}{2a^2} \right) \mathrm{erf}(a) + \frac{1}{a\pi^{\frac{1}{2}}} e^{-a^2} \right] \tag{2.5.8}$$

Equation (2.5.8) represents the effective scatter cross section of the nucleus and is the model used in SimpleMCn to choose between scatter and capture when the neutron energy is less than 9 kT.

At this point it would be prudent to explain the reason the nucleus energy is limited, and why this is done with minimal loss in accuracy of the results. In equation(2.5.7), the

integral on the right is proportional to the density function for the target velocity. The equation is simply transformed to the variable x. This density function decreases rapidly as the value of x increases. Referring to Figure 8, as the energy you wish to find increases, the probability of finding a nucleus at that energy decreases rapidly and will eventually be zero. Using the variable x, the total probability of selecting a value above 3 is only 0.00125 of the total distribution. Limiting the x value to 3 means we retain 99.875% of the original probability distribution results. Compared to the amount of computational time that would be saved, this is a minor error in the overall calculation and in the final result.

We now have the energy of the nucleus and the effective cross section, so next we will need to find the cosine of the direction vectors for which the scatter will take place. This can be obtained by manipulation of equation (2.5.7) to find:

$$f\left(\mu_t\right) = C\left(a^2 + x^2 - 2ax\mu_t\right)^{\frac{1}{2}} \tag{2.5.9}$$

which can be sampled analytically using:

$$\mu_t = \frac{1}{2ax}\left(a^2 + x^2 - \left\{\left|a-x\right|^3 - \xi\left[\left|a-x\right|^3 - \left(a+x\right)^3\right]\right\}^{\frac{2}{3}}\right) \tag{2.5.10}$$

This direction cosine and uniformly sampling an azimuthally angle will fix the direction cosines of the target nucleus (u_t,v_t,w_t). We now have the direction cosines of the incident neutron (u,v,w), and the direction cosines of the target nucleus (u_t,v_t,w_t). In the center-of-mass frame of reference, the scattering is assumed to be isotropic. This means standard collision kinematics are used and the direction of flight for the scattered neutron are sampled

uniformly from a unit sphere (u_o,v_o,w_o). From here we can calculate the final neutron's energy and direction cosines and transform them into the laboratory frame of reference:

$$E' = \frac{E}{(A+1)^2}\left(\bar{x}^2 + \bar{y}^2 + \bar{z}^2\right) \tag{2.5.11}$$

where:

$$u' = \frac{\bar{x}}{\left(\bar{x}^2 + \bar{y}^2 + \bar{z}^2\right)^{\frac{1}{2}}} \tag{2.5.12}$$

$$v' = \frac{\bar{y}}{\left(\bar{x}^2 + \bar{y}^2 + \bar{z}^2\right)^{\frac{1}{2}}} \tag{2.5.13}$$

$$w' = \frac{\bar{z}}{\left(\bar{x}^2 + \bar{y}^2 + \bar{z}^2\right)^{\frac{1}{2}}} \tag{2.5.14}$$

Above:

$$\bar{x} = u + A\left(\delta u_o + \frac{x}{a}u_t\right) \tag{2.5.15}$$

$$\bar{y} = v + A\left(\delta v_o + \frac{x}{a}v_t\right) \tag{2.5.16}$$

$$\bar{z} = w + A\left(\delta w_o + \frac{x}{a}w_t\right) \tag{2.5.17}$$

and

$$\delta = \left(1 + \frac{x^2}{a^2} - \frac{2x\mu_t}{a}\right)^{\frac{1}{2}} \tag{2.5.18}$$

While the above description contains all the information necessary to develop the free gas model, it may be difficult to follow each of the necessary steps. For this, it may be easier to follow the flow diagram in Figure 11 by Carter and Cashwell showing all the steps necessary to find the neutron's scatter energy and direction cosines. Equation (2.5.10) is used in SimpleMCn to find the scatter angle of the thermal scatter. Then equations (2.5.11)-(2.5.14) are used to find the scatter energy and final direction cosines of the scattered neutron.

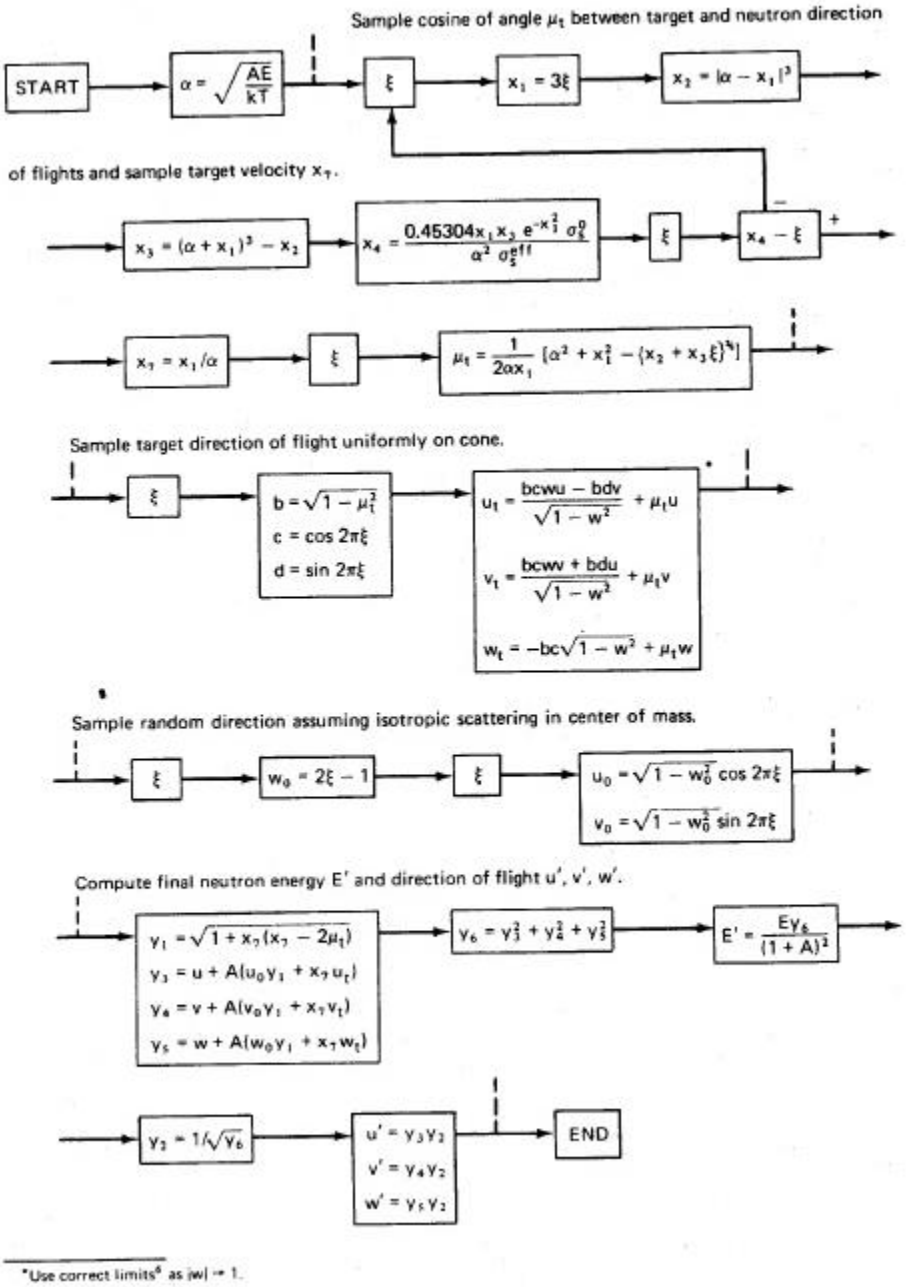

Figure 11 Flow chart from Carter and Cashwell [18] for the free gas treatment of neutrons.

2.6 Biasing Options

The following section discusses several basic biasing techniques used in MC radiation transport simulation to reduce computation time while still preserving the expected value of the results. Biasing methods generally exploit features of geometry, radiation interaction, or weight to drive particle histories toward a desired condition. For this exploitation to work, the property of weight, which determines the particles' contribution to the tally, is adjusted to reflect any changes caused by the biasing. In analog simulations the weight is never changed; the particle starts and dies with a weight of 1 and is only terminated if the particle is captured or escapes. However, in biased simulations, the weight is adjusted by the biasing technique for a more efficient calculation.

Remember SimpleMCn/g's goal is to accurately simulate secondary gamma production from the capture of neutrons. The simplest biasing options available that would improve the calculation's efficiency are implicit capture and forced collision. Both of these options end the particle history using a method called Russian roulette. Finally, the point detector used in SimpleMC is a method of estimating the flux at a point without requiring particles to actually reach the point.

2.6.1 Implicit Capture

Implicit capture allows the neutron to continue living by implying a capture at each interaction point, which then creates secondary radiation. The weight of the neutron is lowered by multiplying the current weight with the ratio of the elastic scatter cross section to the total.

$$\omega_n ' = \omega_n \frac{\Sigma_s}{\Sigma_t} \tag{2.6.1}$$

Where Σ_s is the elastic scatter cross section, Σ_t is the total cross section, ω_n is the neutrons pre-interaction weight and ω_n' is the weight, after implicit capture.

The physical analogy to this operation is that a fraction of the interacting neutron is captured and the remaining fraction scatters [21]. The scattered neutron fraction continues to contribute to the overall history of the MC simulation with the new weight assignment given in equation(2.6.1), while the captured fraction produces secondary gammas with a weight assignment given in equation(2.6.2).

$$\omega_y = \omega_n \frac{\Sigma_c}{\Sigma_t} \tag{2.6.2}$$

Where Σ_c is the capture cross section, ω_y is the photon weight assignment, and ω_n is the neutron weight before implicit capture.

SimpleMC uses implicit capture; however since photons do not lead to secondary radiation, the method is simply used to keep the photon history going within the slab, allowing for a greater chance for escape. The weight is adjusted in the same manner the neutron weight is in SimpleMCn:

$$\omega_y ' = \omega_y \left(1 - \frac{\Sigma_p}{\Sigma_t} \right) \tag{2.6.3}$$

Where Σ_p is the photoelectric absorption cross section, ω_y is the pre interaction gamma weight and ω_y' is the weight after implicit capture.

After applying the change in weight, the photon may either Compton scatter or go through pair production.

2.6.2 Russian Roulette

Russian roulette is method of terminating the history of a particle early, principally since the particle's weight will never reach a weight of zero when implicit capture is employed. The concept is to set a threshold for the minimum weight that a particle is allowed to reach [21]. In SimpleMCn/g, when the particle's weight drops below this threshold, the weight of the particle is either restored to the original weight, or the particle's history is terminated. This termination utilizes a random number ξ, and the ratio of the current weight to the starting weight:

$$\xi < \frac{\omega}{\omega_o} \tag{2.6.4}$$

where ω is the current particle weight and ω_o is the starting weight.

If the condition in (2.6.4) is met, then the particle's weight is reset to ω_o and continues with the rest of its properties unchanged (position, energy, etc.). If the condition is not met, then the particle dies and any related tallies are scored before starting a new history [12]. In this way, SimpleMCn/g can produce the same expected tallies obtained by the analog simulation, while spending less computational time on particles with weights that are so low they are unlikely to contribute to the tally.

2.6.3 Forced Collisions

Forcing collisions is a biasing method meant for optically thin transport media. An optically thin case is considered to be 1 mean free paths or less in thickness [21]. In these model cases, most of the particles will pass through the material before interacting in the material. The developer can either add more trials to the MC simulation or implement the forced collision biasing option. This biasing option keeps the particle from physically escaping the material, generating a fraction of the particle that would escape and a fraction that stays within the transport medium. The fraction that stays within the slab continues to contribute to the particle history, increasing the number of interactions and thus contributing to the tally [19].

This is implemented in SimpleMCn/g by adjusting the distance at which the interaction can be sampled and forcing the particle to interact in the slab. The particle fraction, $\omega^{\dagger}$, that would escape the slab in the particle's current direction is the weight of the particle multiplied by escape probability:

$$\omega^{\dagger} = \omega_o e^{-\Sigma_t D} \tag{2.6.5}$$

where D is the maximum distance the particle can travel and remain in the medium in its current direction and ω_o is the original particle weight.

Therefore the collided fraction and thus new weight is given by:

$$\omega^{*} = \omega(1 - e^{-\Sigma_t D}) \tag{2.6.6}$$

where ω^{*} is the particle weight after applying the forced biasing option

Since the interaction is now forced to occur within distance D, a new method is needed to select the interaction distance L. A ratio is formed of the probability of interacting within a distance L and the allowable distance D, and the random number ξ represents that ratio:

$$\xi = \frac{P(\mathrm{L})}{P(\mathrm{D})} \tag{2.6.7}$$

where,

$$P(\mathrm{L}) = 1 - e^{-L\Sigma_t} \tag{2.6.8}$$

and

$$P(\mathrm{D}) = 1 - \mathrm{e}^{-D\Sigma_t} \tag{2.6.9}$$

Solving for L, equation (2.3.3) is replaced by the following equation to determine the forced interaction distance:

$$L = -\frac{\ln(1 - \xi(1 - \mathrm{e}^{-\Sigma_t D}))}{\Sigma_t} \tag{2.6.10}$$

2.6.4 Point Detector Tally

In order to estimate a detector's response at a particular location, the flux must be estimated at that location. The point detector tally works by estimating the likelihood that a scattering photon will reach the detector's position. The weight that the detector records is adjusted to reflect the probability of scattering into the direction of the detector, and to travel through the material without any interactions [19].

The probability of the particle scattering towards a non-point detector is:

$$p(\vec{\Omega}_p)d\vec{\Omega}_p \tag{2.6.11}$$

where $\vec{\Omega}_p$ is the direction vector from the collision to the detector and $d\vec{\Omega}_p$ is the solid angle subtended by the detector.

The probability of reaching the detector without a collision is:

$$e^{-\int_0^R \Sigma_t(s)ds} \tag{2.6.12}$$

where R is the distance between the interaction point and the point detector.

Combining these two factors yields the probability that the particle will scatter towards the detector and reach it uncollided:

$$p(\vec{\Omega}_p)d\vec{\Omega}_p e^{-\int_0^R \Sigma_t(s)ds} \tag{2.6.13}$$

Now inserting the weight of the incident particle and reducing the detector size to zero:

$$tally = w\frac{p(\vec{\Omega}_p)}{r^2}e^{-\int_0^R \Sigma_t(s)ds} \tag{2.6.14}$$

The azimuthal component of the scatter direction is uniformly distributed, so equation (2.6.14) becomes:

$$tally = w\frac{p(\mu)}{2\pi r^2}e^{-\int_0^R \Sigma_t(s)ds} \tag{2.6.15}$$

where μ is the cosine of the polar angle.

For photons, p(μ) is determined by the Klein-Nishina cross-section using either Kahn rejection or Koblinger direct sampling.

CHAPTER 3

Results

The process of confirming the operation of SimpleMCn/g was to tally neutron and gamma reflection and transmission in:

1. radial location
2. polar angle with respect to the slab normal
3. azimuthal angle with respect to the x-axis
4. emergent energy distributions

SimpleMCn/g tallies were compared to the same tallies from MCNP. See Figure 10 for an illustration of these tallies. It is important to note that the radial tallies are set from the entry point of the neutron beam. The polar and azimuthal angles are binned with respect the exit location of the escaping particle. Since the primary goal of this thesis is to produce secondary gamma rays in a computationally efficient way, the number of photons produced per neutron history was also recorded to compare the efficiency of the biasing options and demonstrate their effectiveness.

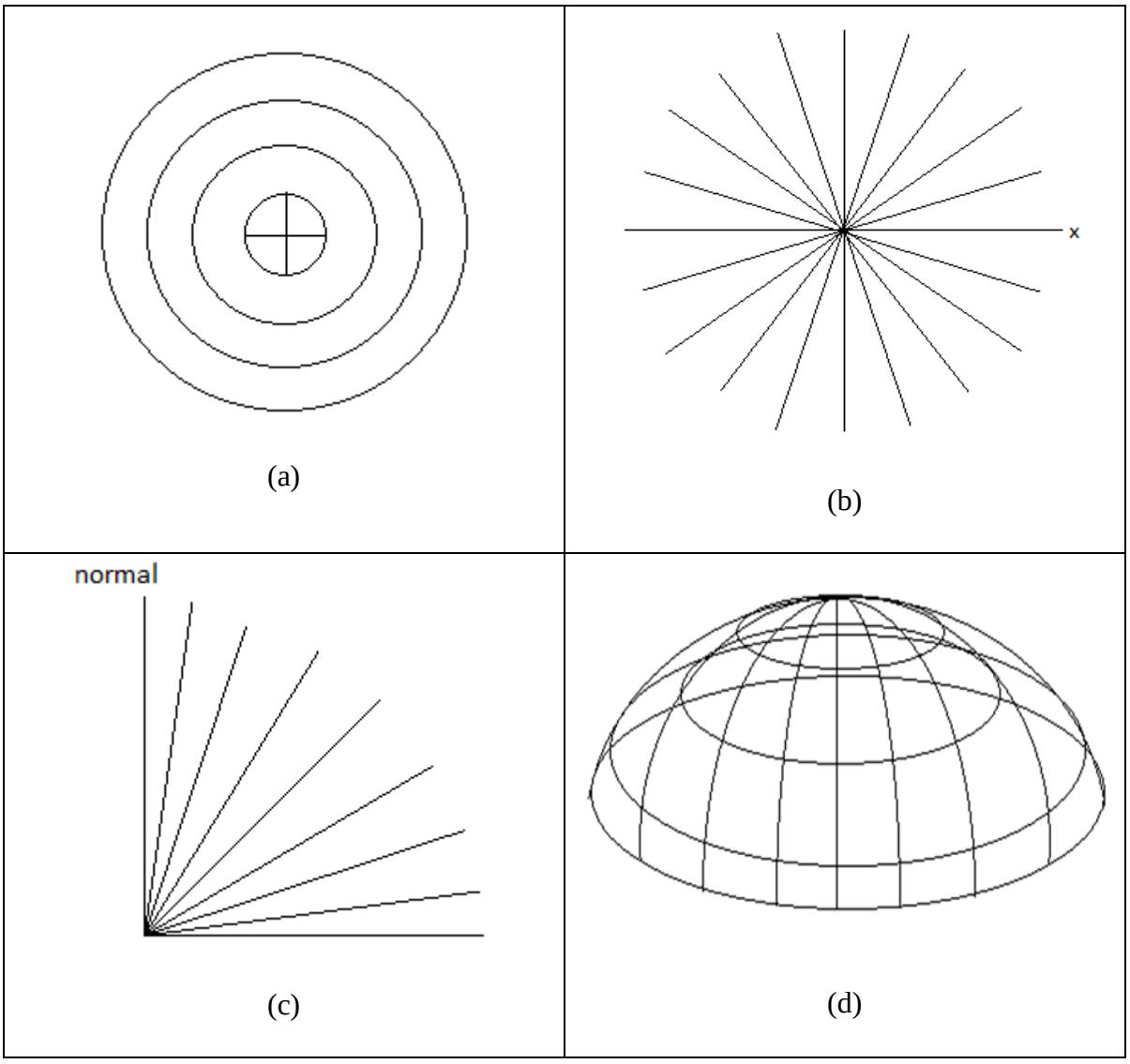

Figure 12 Illustraion of the (a) radial distribution, where the cross hairs represent the entry point of the source neutrons into the slab, and the (b) azimuthal and (c) polar binning of the emerging particles. (d) a 3-d representation of the polar and azimuthal binning, which occur at the location the particle exits the slab.

At the start of the project, there was a discrepancy between the analog sets of neutron tallies, indicating that the neutrons in SimpleMCn were not “living” as long as the neutrons

in MCNP. The tallies, shown in Figure 13, for SimpleMCn were much lower than those of MCNP, except for in energy. For the energy distribution, the reflected tallies at higher energies are practically the same, but differed greatly at lower energies. Where MCNP exhibits a local maximum in the neutron spectrum near 0.01 eV, SimpleMCn immediately begins to fall off. This was an indication that thermal neutron scattering wasn't adequately modeled in SimpleMCn, and this missing physics was responsible for a longer life of these neutrons in MCNP. The effects of this on the secondary gammas are shown in Figure 12.

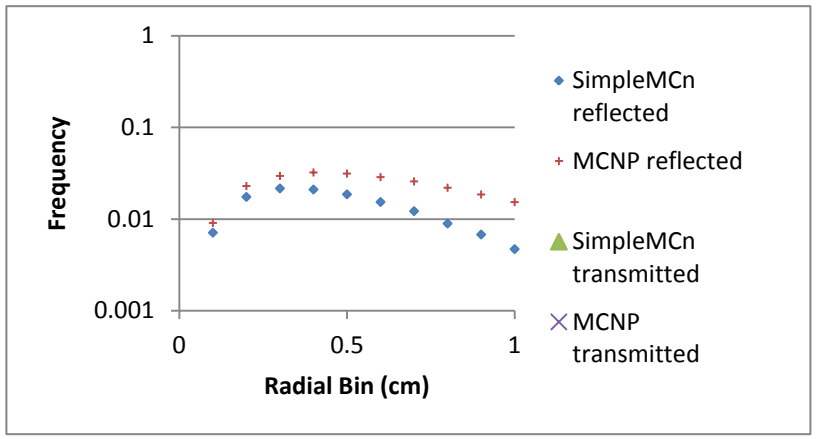

(a)

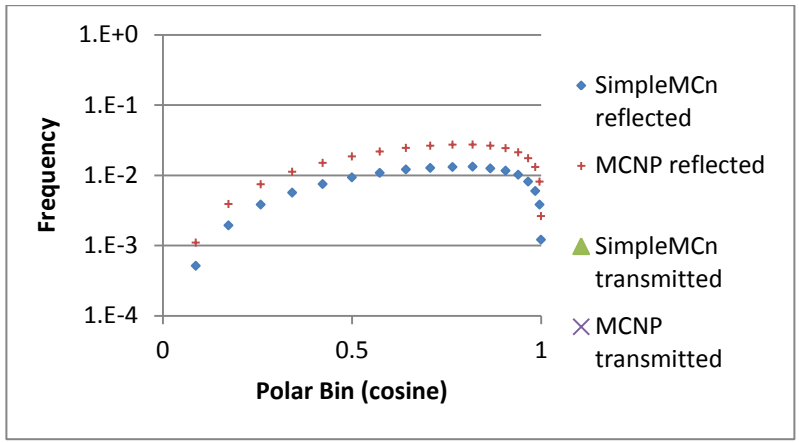

(b)

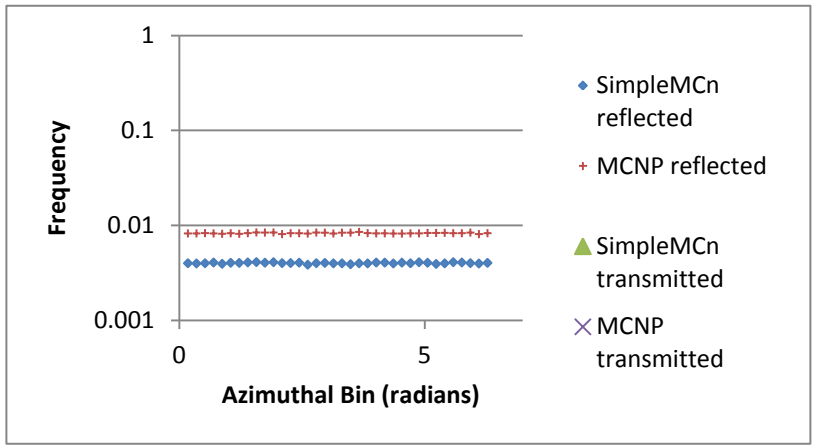

(c)

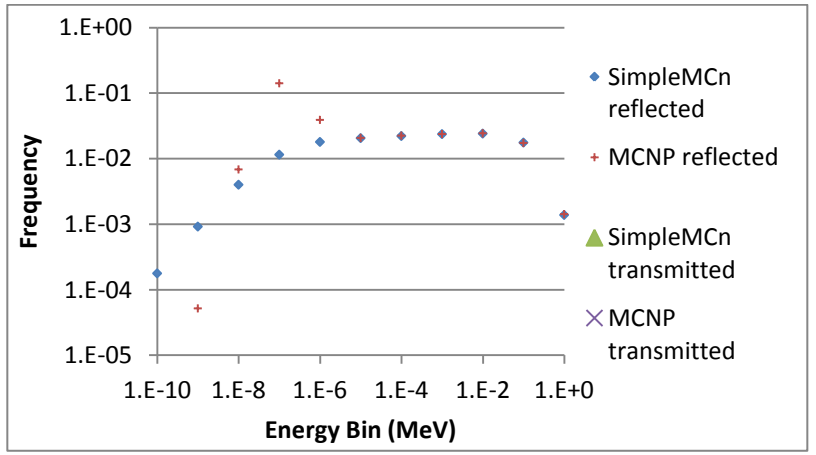

(d)

Figure 13 The (a) radial, (b) polar, (c) azimuthal, and (d) energy distribution of the neutrons from SimpleMCn before the thermal treatment of the neutrons. Note the discrepancy for the neutrons at low energy.

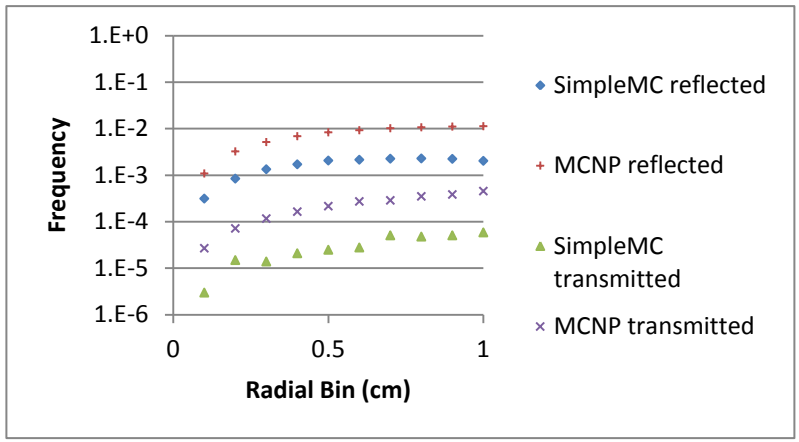

(a)

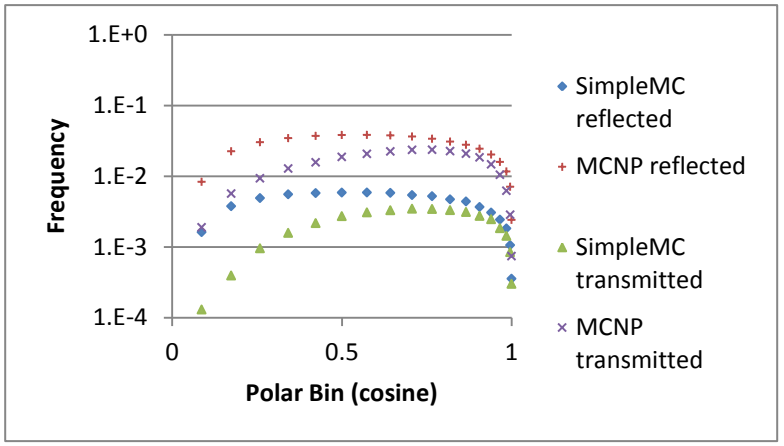

(b)

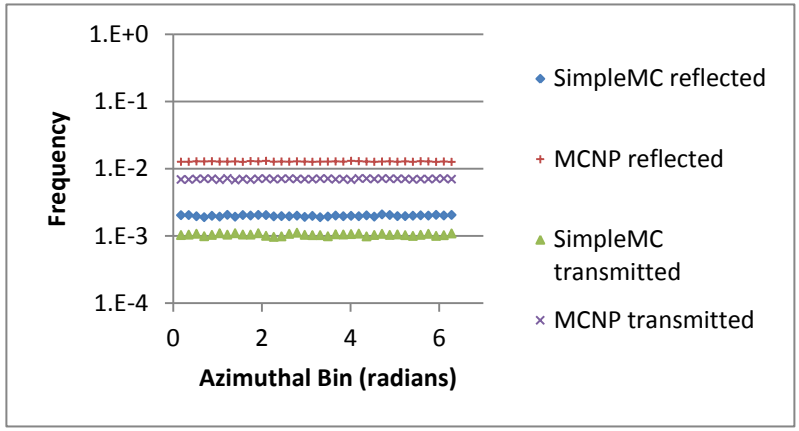

(c)

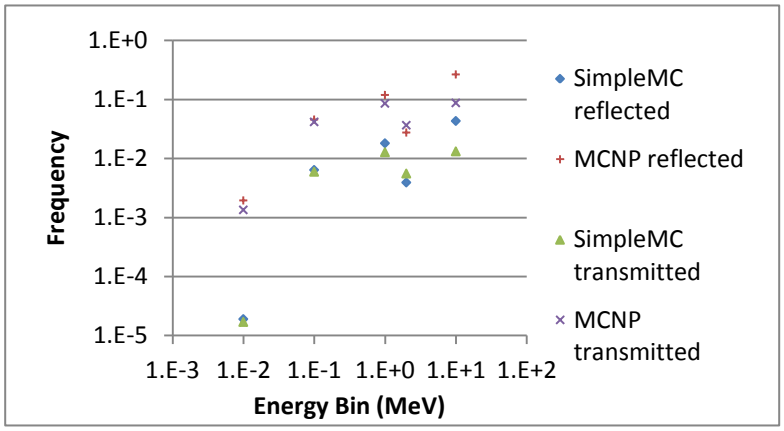

(d)

Figure 14 The (a) radial, (b) polar, (c) azimuthal, and (d) energy distribution of the photons from SimpleMC before the thermal treatment of neutrons in SimpleMCn.

After identifying that the issue was with the treatment of thermal neutrons [18], the free gas treatment of neutrons, covered in section 2.5.2a, was discovered and applied in SimpleMCn. The resulting analog distributions became identical for both the neutrons in Figure 13, and the photons in Figure 14. The issue with the transmitted neutron tallies in Figure 13 is that SimpleMCn does not employ a lower energy level cutoff limit, where MCNP does. The transmitted results are from neutrons with energies less than the MCNP energy cutoff of $1*10^{-11}$ MeV. For this analog test case, SimpleMCn produces 0.446 photons per neutron history. Figures 13-14 confirm that the analog treatment of neutrons in SimpleMCn and the coupling of secondary photons with SimpleMC is functioning correctly.

Note that with the geometry of the problem (a beam of neutrons directly into a slab), the azimuthal distribution is expected to be, and is, an entirely flat distribution.

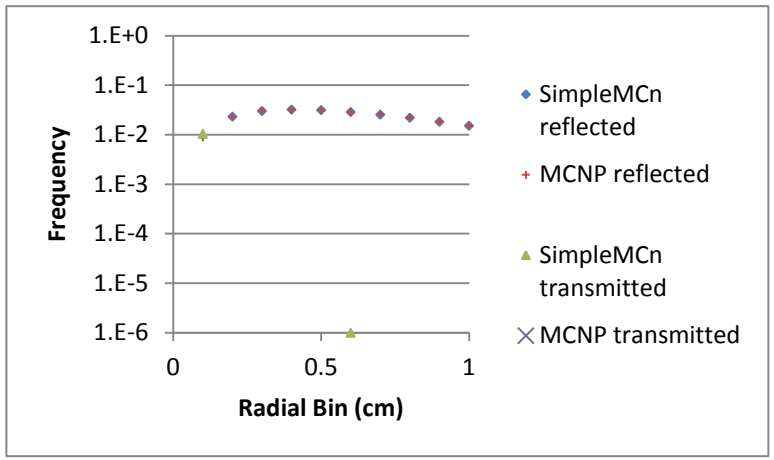

(a)

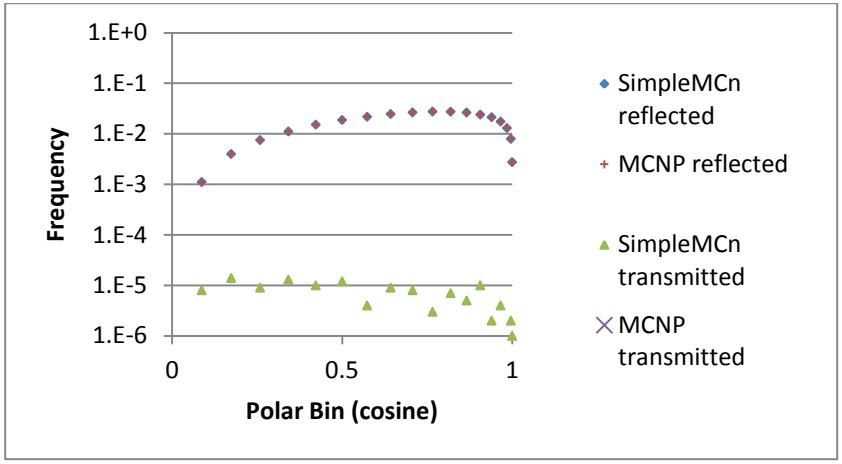

(b)

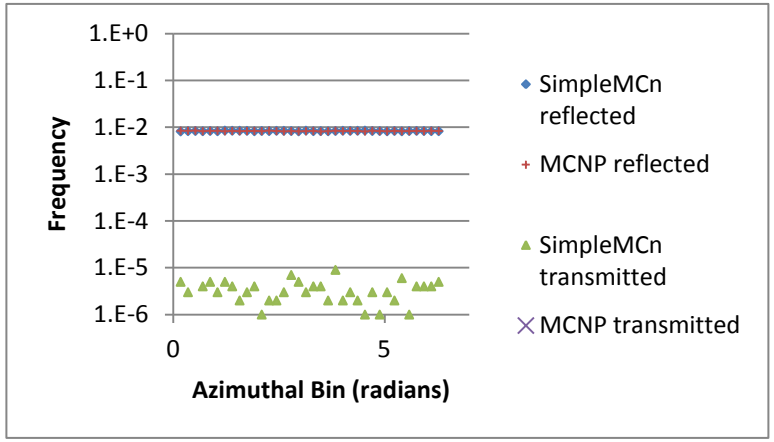

(c)

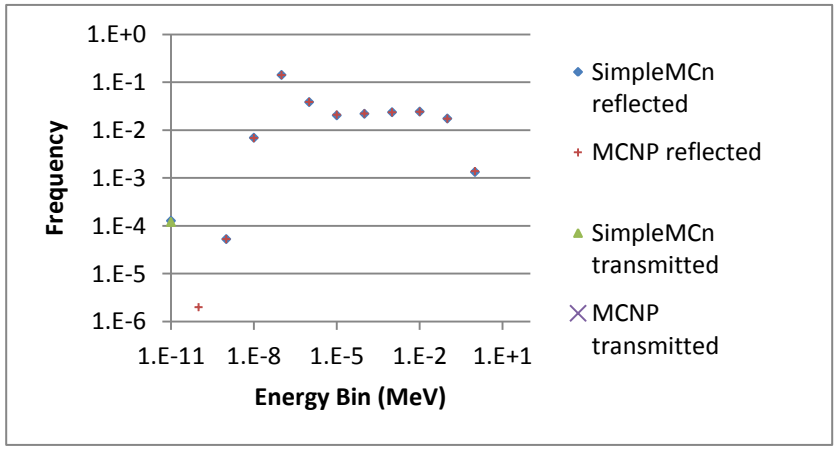

(d)

Figure 15 The (a) radial, (b) polar, (c) azimuthal, and (d) energy distributions of neutrons from SimpleMCn after the free gas treatment of neutrons

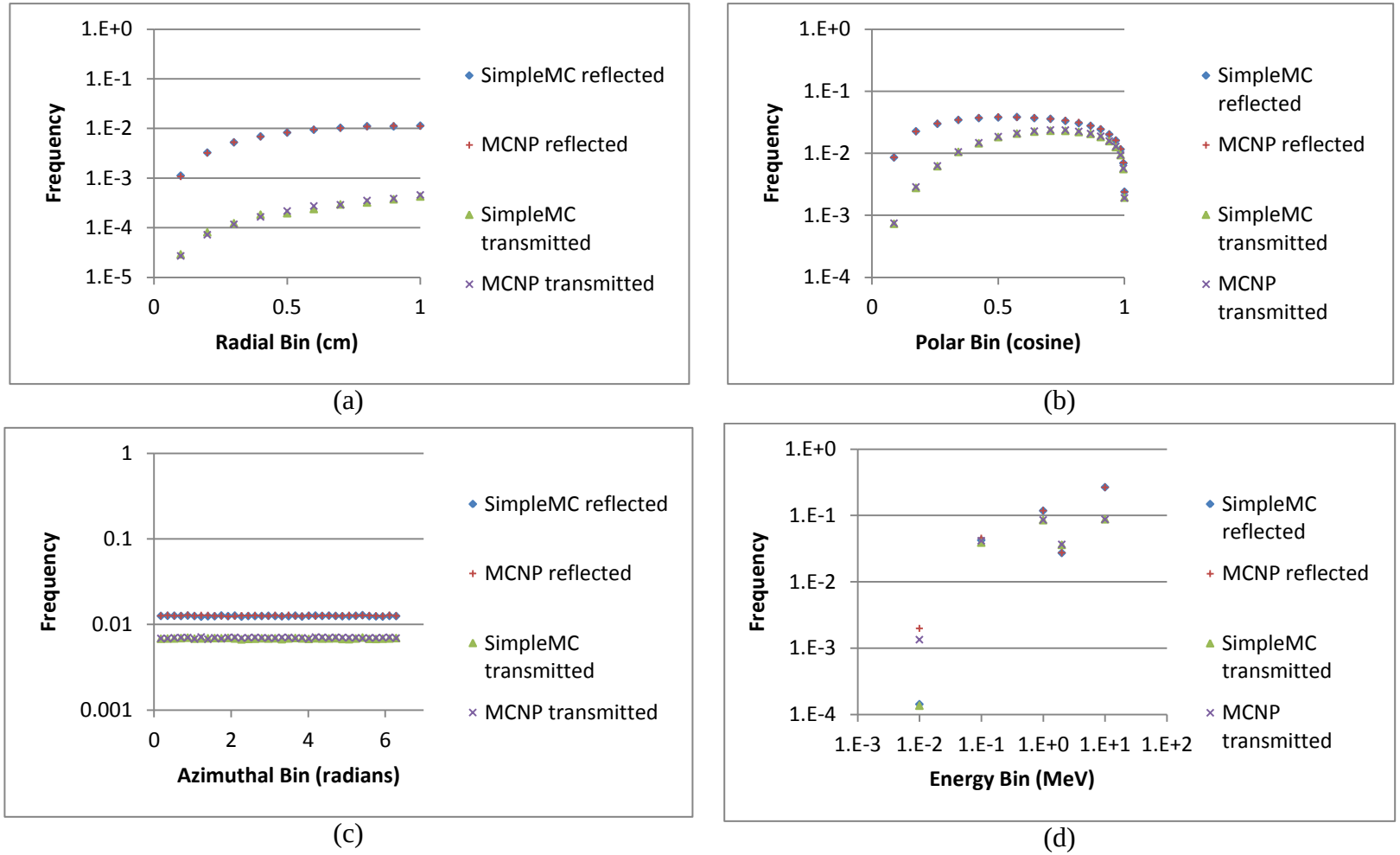

Figure 16 The (a) radial, (b) polar, (c) azimuthal, and (d) energy distributions of photons from SimpleMC using input from SimpleMCn after the application of the free gas treatment on thermal neutrons.

The next step is to test, in the same manner, the different neutron biasing options to ensure that they produce the same tallied results. First is the implicit capture of neutrons, shown in Figure 15. Again, the distributions for the reflected neutrons are equivalent The issue of the optically thick slab persists in the MCNP results. This provides confirmation that the neutron histories are properly simulated with implicit capture. The number of photon histories produced is increased to 148.785 photons per neutron. This is a factor of 333 increase in the production of photons over the analog case, which shows that implicit capture is an effective biasing option for the production of secondary gamma rays.

The results for the secondary gammas, which were modeled using analog transport, are presented in Figure 16. The photon distributions are equivalent to the MCNP results, proving that not only are the neutron histories being simulated correctly with implicit capture, but that the photon production from this method is correct.

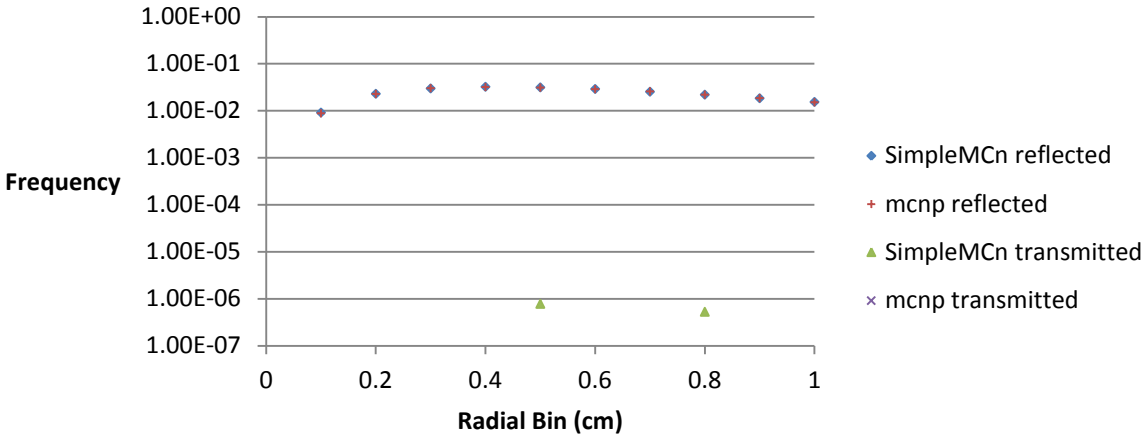

(a)

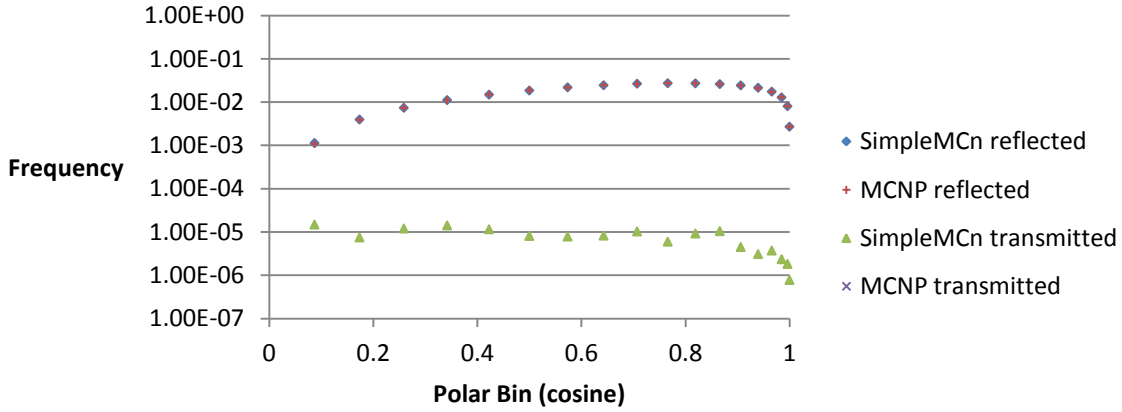

(b)

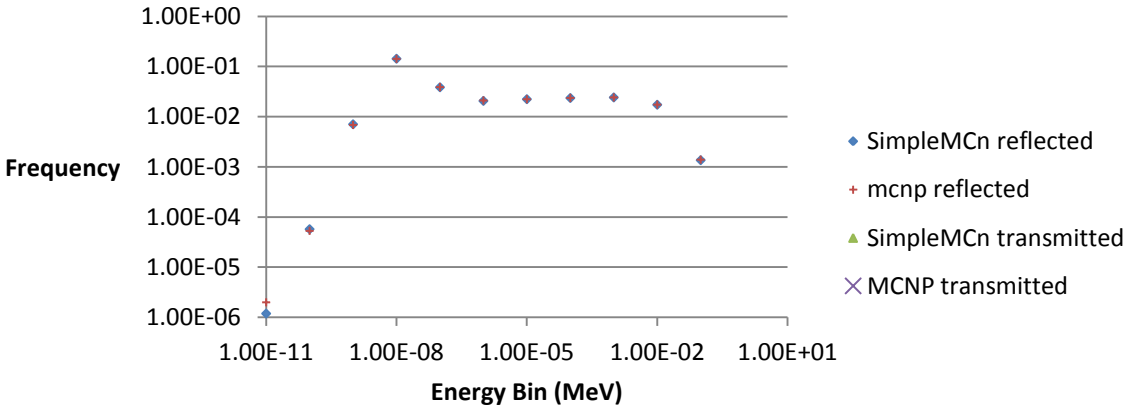

(c)

Figure 17 The (a) radial, (b) polar, and (c) energy distributions of neutrons from SimpleMCn using implicit capture.

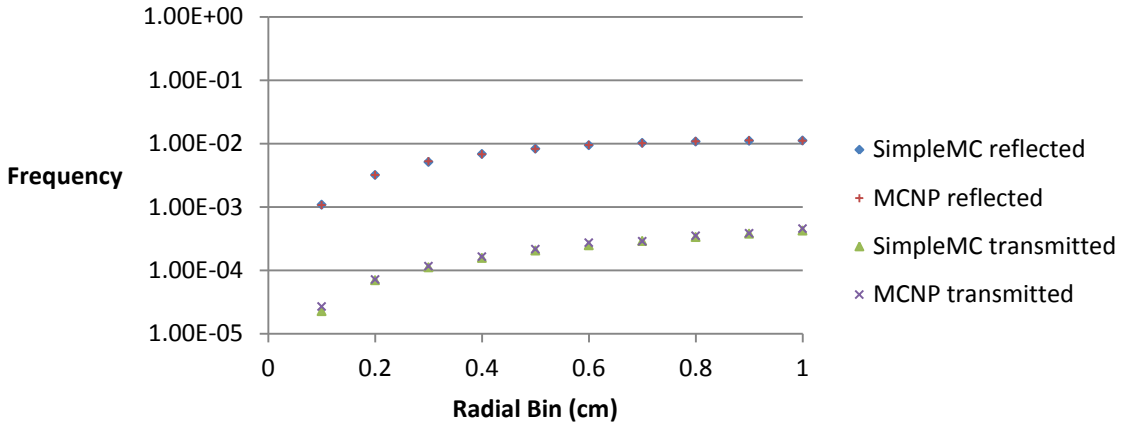

(a)

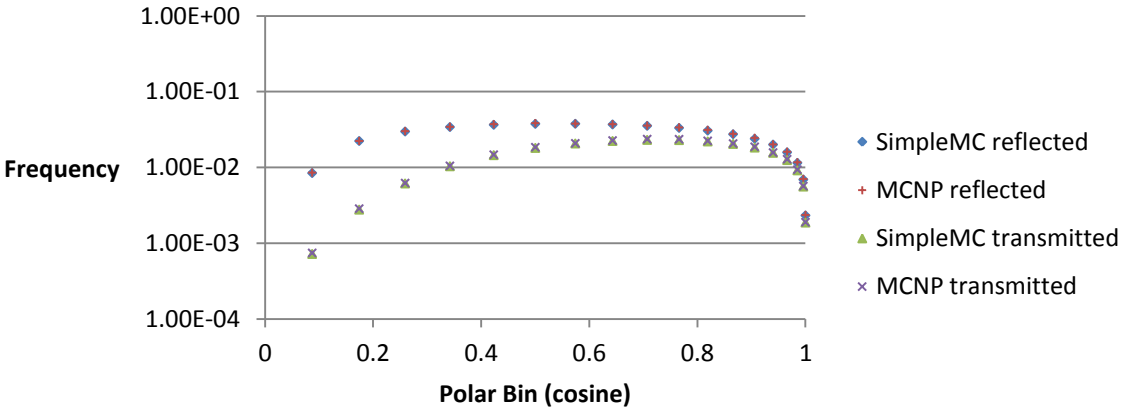

(b)

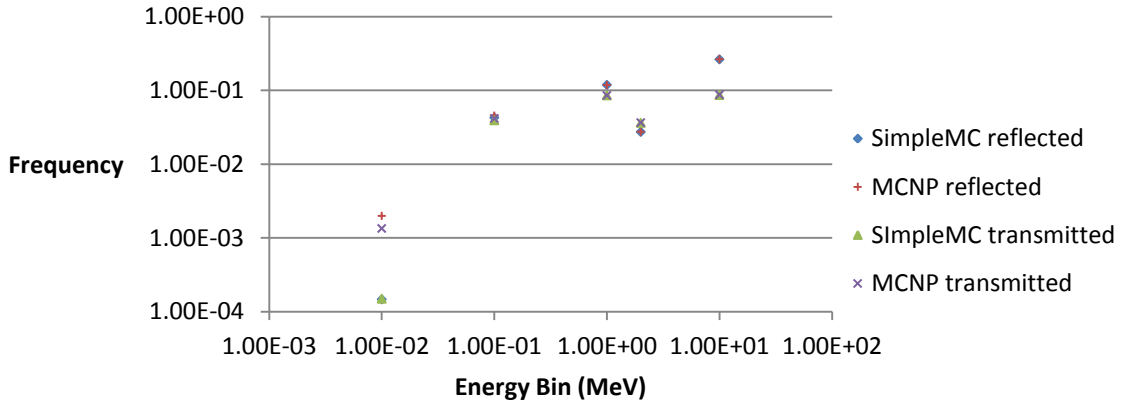

(c)

Figure 18 The (a) radial, (b) polar, and (c) energy distributions of photons from SimpleMC using input from SimpleMCn using implicit capture.

For the forced collision option, the 10 cm thick slab with a density of 1 g/cc was too optically thick for the neutrons. In order to properly test the selection of a forced distance within the slab, the neutrons needed to have a high probability of escaping uncollided. This meant the optical thickness needed to be adjusted, and so the density was lowered to about three percent of the original value, 0.03 g/cc, so that the slab was approximately 1 mean free path for the neutrons.

With this reduction of optical thickness, the number of analog neutron tallies dropped significantly, from 0.446 photons per neutron to 0.003 photons per neutron. However, the forced collision biasing for 1 mean free path resulted in an increase to 0.008 photons per neutron, which is a 1.5 factor increase in the number of secondary photons produced in analog simulation. While not as large an increase as the implicit capture biasing, it is important to remember that the use of forced collision biasing is intended for optically thin media.

The SimpleMCn neutron distribution tallies using forced collision biasing are shown in Figure 17; note that the MCNP data is from an analog simulation. One can see that both the reflected and transmitted data match with MCNP, meaning the forced option is correctly simulated and that using 1 mean free path has allowed both MCNP and SimpleMCn to tally transmission data. Figure 18 displays the photon data from SimpleMC, and though the numbers of photons tallied are low, the tallies match the MCNP results in the polar and energy distributions.

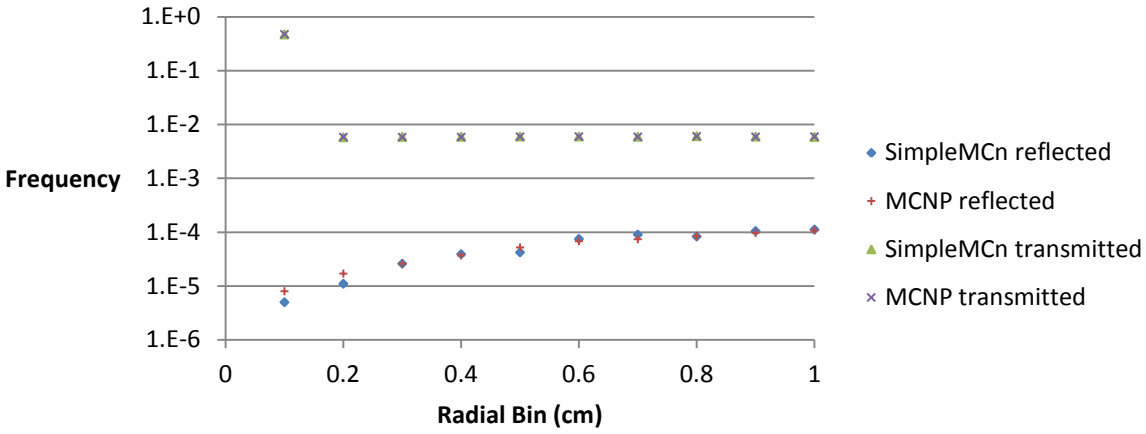

(a)

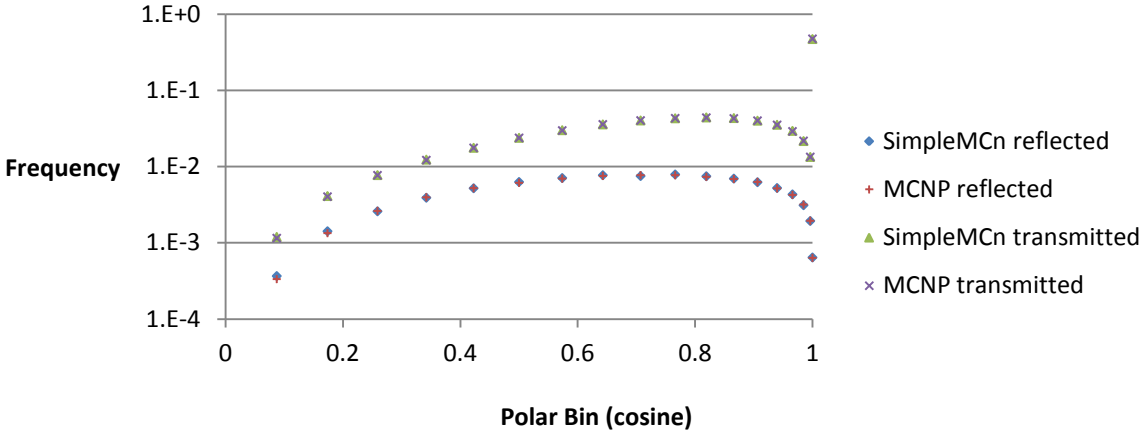

(b)

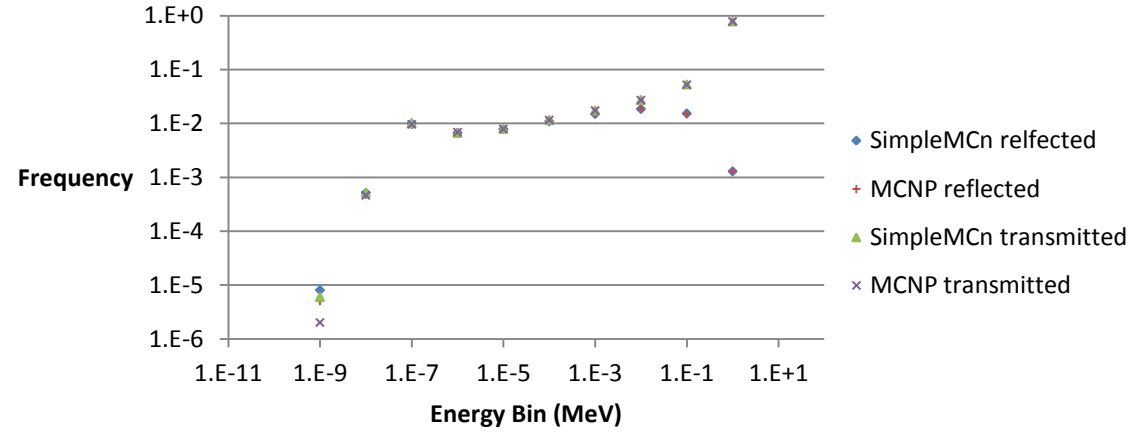

(c)

Figure 19 The (a) radial, (b) polar, and (c) energy distributions of neutrons from SimpleMCn using the forcing biasing option.

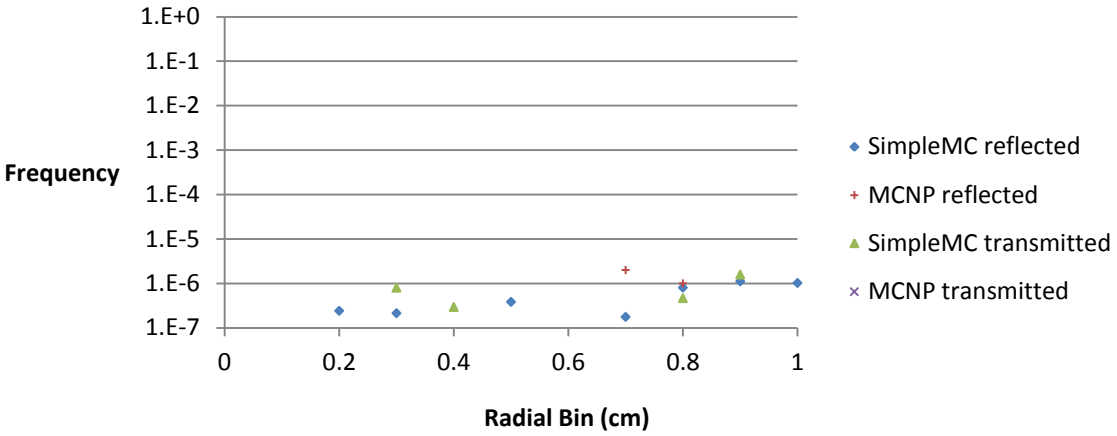

(a)

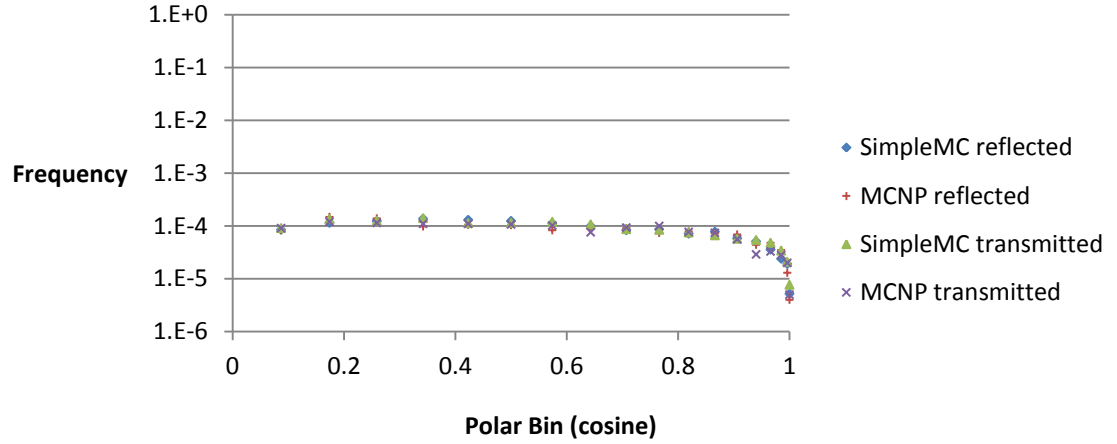

(b)

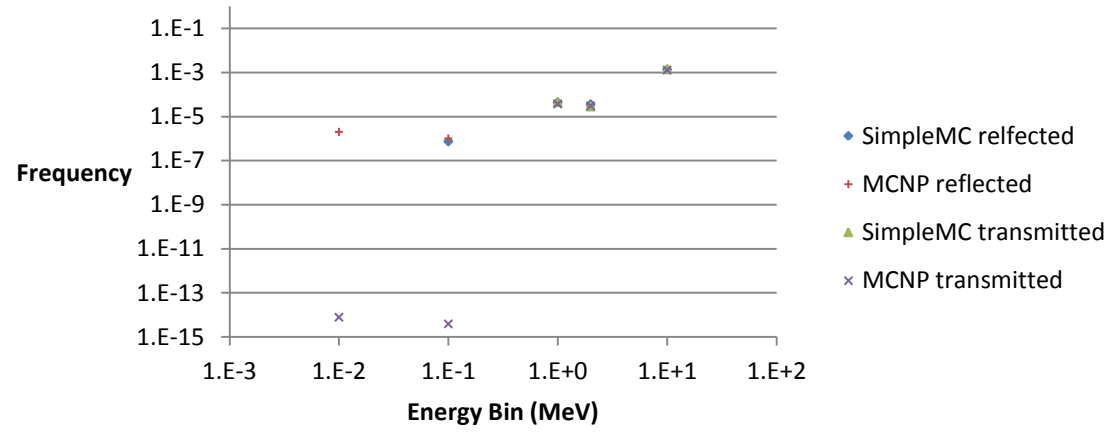

(c)

Figure 20 The (a) radial, (b) polar, and (c) energy distributions of photons from SimpleMC using input from SimpleMCn with forcing.

Table 3.1 compares the numerical results of implementing the biasing options in SimpleMCn/g. Note that the results are in either gammas per neutron or gammas per second. Also, for the displayed run times, a standard desktop computer with the clock speed time of 3.1 GHz.

Table 3.1: Summary of photon histories from analog and biasing options

Optical Setting	Analog (γ/n)	Run Time (γ/s)	Implicit Capture (γ/n)	Run Time (γ/s)	Forced (γ/n)	Run Time (γ/s)
Optically Thick	0.446	334	148.785	11700	N/A	N/A
Optically Thin	0.003	75	N/A	N/A	0.008	95

The last test to check is the point detector using photons generated from SimpleMCn. The detector is placed 100 cm away from the neutron entry point, at a 45^{o} angle form the normal. This results in the x-y-z coordinates of 0.0, 70.71068, 70.71068. Since 2.223 MeV photons are the highest energy photons that are produced in SimpleMCn, the point detector is set to 100 bins, evenly divided from 0 to 2.223 MeV. The results are shown in Figure 21.

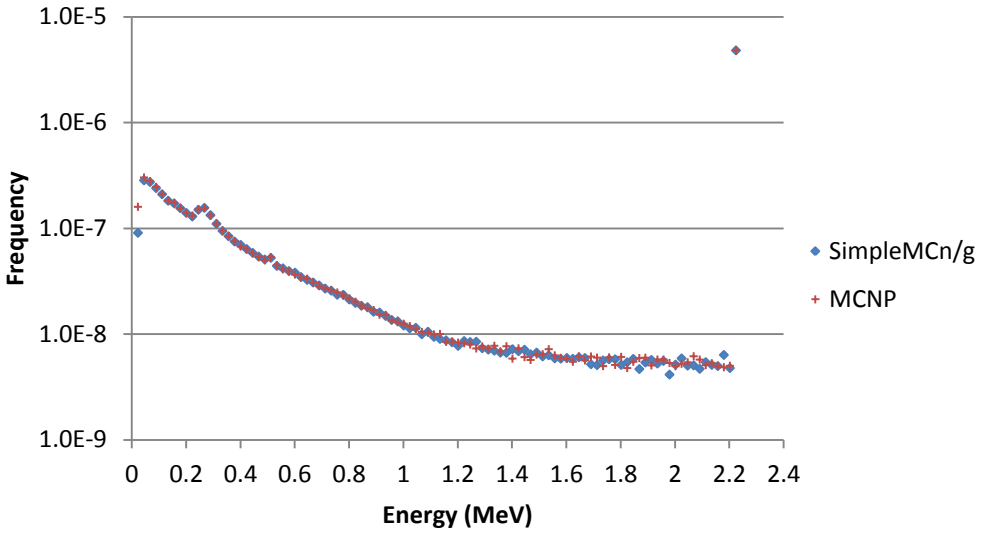

Figure 21 Point detector tally for photons from SimpleMCn/g. Both the neutrons and photons were analog treated.

As one can see, the point detector results are nearly identical to MCNP. The slight discrepancy at lower energies is from the fact that the Klien-Nishina model breaks down at low energies due to Doppler broadening of the electron [19].

CHAPTER 4

Conclusion

The preceding results demonstrate that SimpleMCn is able to simulate neutron transport as well as efficiently producing secondary gamma rays from neutron capture, a principle goal of this work. The results also demonstrate that the coupling of photons generated from SimpleMCn with SimpleMC is functioning accurately. With the test case provided, the analog, implicit capture and forced collision cases matched the MCNP benchmark results. In addition, the implicit capture method increased the number of secondary gammas by a factor of 333 and the forced collision method increased their production by a factor of 1.5.

Matching the analog results of SimpleMCn/g and MCNP demonstrates that the physical simulation of the neutrons and photons are correctly modeled. The matching results for the biasing options shows that these methods are correctly implemented in SimpleMCn. These results, in conjunction with the fact that the implicit capture and forced collision biasing options increase the number of secondary gammas, confirm that SimpleMCn is capable of efficiently simulating secondary gamma production from neutron capture.

4.1 Future Work

There are several aspects of SimpleMCn and SimpleMC that need to be developed before it can complete the overall goal of real-time training simulation. The most important feature would be to develop the programs so that they may be interfaced to a computer aided drafting (CAD) program. The data provided by these two programs would be used to

generate the radiation field in the built environment much like light is rendered in computer programs. In order to reach this point, both SimpleMCn and SimpleMC would need to be combined into one integrated program that could be attached to an already developed CAD program. In order for this to be viable, the integrated program will also need to be rewritten in to a language designed for graphics processing units (GPU), such as CUDA. While the programs operate correctly individually, there is a user benefit to making one integrated program that executes a single coupled transport simulation.

In addition, both SimpleMCn and SimpleMC will need to have their cross sections restructured. Currently, cross-sections are hard coded into both programs. SimpleMC has the macroscopic cross sections hardcoded. This means that the user will need to manually change the photon cross sections every time they wish to make run with a new density of the material. Since more materials will be added to the programs in the future, having to keep the cross sections added to the program would mean extra data that would need to be downloaded with the program. Ideally, the goal would be to have a section of the program pull the relevant cross section data from an online source like ENDF or XCOM, but that work is beyond the current scope of this thesis.

Another subject that would need to be developed for the future coupled SimpleMCn/g program is the addition of detector response. While the point detector in SimpleMC will find the flux impingent on a detector at an arbitrary location in the environment, it will not directly correlate to the detector's response. There are multiple types of detectors each exploiting one of many different detection methods. These different methods respond

differently, even if the radiation flux on them is the same. In simulations, the radiation flux is converted into the detector response through models known as detector response functions. These detector response functions will need to be added into the coupled SimpleMCn/g program if the user wishes to train personnel using actual detectors available to the trainees.

REFERENCES

[1] **C. J. Everett, E. D. Cashwell.** *A Monte Carlo Sampler.* Springfield : National Technical Information Service, 1972.

[2] —. *A Second Monte Carlo Sampler.* Springfield : National Technical Information Service, 1974.

[3] **J. K. Shultis, R. E. Faw.** *Radiation Shielding.* s.l. : American Nuclear Society, 2000.

[4] *Direct Sampling from the Klien-Nishina Distribution for Photon Energies Above 1.4 MeV.* **Koblinger, L.** 2, s.l. : Nuclear Science and Engineering, 1975, Vol. 56.

[5] **Khan, H.** *Applications of Monte Carlo.* Springfield : National Technical Information Services, 1956.

[6] *Random Number Generators: Good Ones are Hard to Find.* **S. K. Park, K. W. Miller.** 10, s.l. : Communications of the ACM, Vol. 31.

[7] **Schrage, L.** A More Portable Fortran Random Number Generator. *ACM Transactions on Mathematical Software.* 1979, Vol. 5, 2.

[8] **W. H. Press, S. A. Teukolsky, W. T. Vetterling, B. P. Flannery.** *Numerical Recipes in C++*. Cambridge : The Press Syndicate of the University of Cambridge, 2002.

[9] **C. Bays, S. D. Durham.** Improving a Poor Random Number Generator. *ACM Transactions on Mathematical Software.* 1976, Vol. 2, 1.

[10] *Efficient and Portable Combined Ranndom Number Generators.* **L'Eculyer, P.** 6, s.l. : Communications of the ACM, Vol. 31.

[11] **B. Carnahan, H. A. Luther, J. O. Wilkes.** *Applied Numerical Methods.* New York : John Wiley & Sons, 1969.

[12] **I. Lux, L. Koblinger.** *CRC Monte Carlo Particle Transport Methods: Neutron and Photon Calculations.* Boca Raton : CRC Press, 1991.

[13] **Lewis, E. E.** *Fundamentals of Nuclear Reactor Physics.* Burlington : Academic Press, 2008.

[14] **J. J. Duderstadt, L. J. Hamilton.** *Nuclear Reactor Analysis.* s.l. : John Wiley and Sons, 1976.

[15] **N. Tsoulfanidis, S. Landsberger.** *Measurement and Detection of Radiation.* Boca Raton : CRC Press, 2011.

[16] **Knoll, G. F.** *Radiation Detection and Measurement.* s.l. : Johm Wiley & Sons, 2010.

[17] **E. D. Cashwell, C. J. Everett.** *A Practical Manual on the Monte Carlo Method for Random Walk Problems.* New York : Pergamon Press, 1959.

[18] **L. L. Carter, E. D. Cashwell.** *Particle-Transport Simulation with the Monte Carlo Method.* s.l. : Technical Information Center Energy and Development Adiminstration, 1975.

[19] **Team, X-5 Monte Carlo.** *MCNP — A General Monte Carlo N-Particle Transport Code, Version 5.* s.l. : Los Alamos National Laboratory, 2008.

[20] **Knuth, D. E.** *The Art of Computer Programming.* Upper Saddle River : Addison-Wesley, 2011.

[21] **S. A. Dupree, S. K. Fraley.** *A Monte Carlo Primer.* s.l. : Kluwer Academic/Plenum Publishers, 2002.

[22] **Krane, Kenneth S.** *Introductory Nuclear Physics.* s.l. : John Wiley & Sons, 1988.

[23] **Nuclear Energy Agency.** Janis 4. [Online] Nuclear Energy Agency. http://www.oecd-nea.org/janis/.

[24] **Holmes, J. C.** *Monte Carlo Calculation of Thermal Neutron Inelastic Scattering Cross Section Uncertainties by Sampling Perturbed Phonon Spectra.* Raleigh : North Carolina State University, 2014.